AD_____

Award Number: W81XWH-07-1-0140

TITLE: The Role of Backup NHEJ Repair in Creating Genomic Instability in CML

PRINCIPAL INVESTIGATOR: Feyruz Rassool, Ph.D.

CONTRACTING ORGANIZATION: University of Maryland School of Medicine
Baltimore, MD 21201

REPORT DATE: March 2008

TYPE OF REPORT: Final

PREPARED FOR: U.S. Army Medical Research and Materiel Command
Fort Detrick, Maryland 21702-5012

REPORT DOCUMENTATION PAGE

Form Approved
OMB No. 0704-0188

1. REPORT DATE *(DD-MM-YYYY)*	**2. REPORT TYPE**	**3. DATES COVERED** *(From - To)*
31-03-2008	Final Report	01 MAR 2007 - 28 FEB 2008

4. TITLE AND SUBTITLE"

The Role of Backup NHEJ Repair in Creating Genomic Instability in CML"

5a. CONTRACT NUMBER

5b. GRANT NUMBER
W81XWH-07-1-0140

5c. PROGRAM ELEMENT NUMBER

6. AUTHOR(S)
Feyruz Rassool

5d. PROJECT NUMBER

5e. TASK NUMBER

5f. WORK UNIT NUMBER

7. PERFORMING ORGANIZATION NAME(S) AND ADDRESS(ES)

University of Maryland School of Medicine
655 West Baltimore Street
BRB 7-023A
Baltimore, MD 21201

8. PERFORMING ORGANIZATION REPORT NUMBER

9. SPONSORING / MONITORING AGENCY NAME(S) AND ADDRESS(ES)
US Army Medical Research
And Materiel Command
Fort Detrick, Maryland 21702-5012

10. SPONSOR/MONITOR'S ACRONYM(S)

NUMBER(S)

12. DISTRIBUTION / AVAILABILITY STATEMENT

Approved for public release; distribution unlimited

13. SUPPLEMENTARY NOTES

14. ABSTRACT
This proposal seeks to build on our preliminary data that provides a mechanism for the reduced repair fidelity in BCR-ABL-positive CML. In this scenario, double strand breaks (DSB) produced by increased reactive oxygen species (ROS) in BCR-ABL-positive CML need to be processed before proper repair can occur. However, we find that one key main NHEJ protein responsible for this processing, Artemis, is down-regulated in BCR-ABL-positive CML. Concomitantly, we find upregulation of a **novel complex of proteins**, some of which are known to be involved in a minor "back-up" NHEJ repair pathway. WRN, a protein, which is found deleted in the accelerated aging disease, Werner's syndrome is a newly found constituent of this complex, that contains, DNA Ligase III, XRCC1 and PARP.

We report that:

1. The **novel protein complex** we have identified in CML cells **localizes to DSB**.

2. These proteins repair DSB because their "down-regulation" (a) increases the number of **unrepaired DSB**, and (b) affects the **repair efficiency and fidelity** in CML cells. Overexpression of Artemis, the main NHEJ protein found down regulated in CML cells, increases correct repair of DSB.

3. We have preliminary data that up-regulation of "back-up" repair proteins **is dependent on expression of BCR-ABL**.

Finally, we have a manuscript in revision in a high impact sub-specialty journal, Blood, describing this work (appendix).

15. SUBJECT TERMS Main non homologous end-joining repair (NHEJ) , Back-up NHEJ repair,double strand breaks (DSB),chronic myeloid leukemia (CML)

16. SECURITY CLASSIFICATION OF:			**17. LIMITATION OF ABSTRACT**	**18. NUMBER OF PAGES**	**19a. NAME OF RESPONSIBLE PERSON**
a. REPORT	**b. ABSTRACT**	**c. THIS PAGE**	UU	**70**	USAMRMC
U	U	U			**19b. TELEPHONE NUMBER** *(include area code)*

Table of Contents

Page

Introduction:

Background: We and others have recently shown that the oncogenic BCR-ABL fusion protein in Philadelphia (Ph)-positive CML initiates a cycle of genomic instability that results in the acquisition of further genomic changes that can contributes to disease progression(Melo 1996). BCR-ABL produces increased reactive oxygen species (ROS) that leads to DNA damage, including double strand breaks (DSB) (Sattler et al. 2000). In turn, key facets of genomic instability in cancer and leukemia are caused by alterations in the pathways that repair DSB. We and others have demonstrated significantly increased error-prone repair of DSB in CML cells mediated by the non homologous end-joining (NHEJ) pathway, one of the main pathways for DSB repair in mammalian cells (Gaymes et al. 2002a, Brady et al. 2003). However, the mechanisms biasing for this increased error-prone repair component of NHEJ in BCR-ABL-positive CML has yet to be clarified.

Purpose of Research: This proposal seeks to build on our preliminary data that provides a mechanism for the reduced repair fidelity in BCR-ABL-positive CML. In this scenario, DSB produced by increased ROS in BCR-ABL-positive CML need to be processed before proper repair can occur. However, we find that one key protein responsible for this processing, Artemis, is down-regulated in BCR-ABL-positive CML. Concomitantly, we find upregulation of a novel complex of proteins, some of which are known to be involved in a minor "back-up" NHEJ repair pathway. WRN, a protein, which is found deleted in the accelerated aging disease, Werner's syndrome is a newly found constituent of this complex, that contains, DNA Ligase III, XRCC1 and PARP. We propose that this **novel protein complex** processes and repairs ROS-induced DSB with poor repair fidelity. Furthermore, we intend to verify preliminary data that this repair complex is dependent on expression of BCR-ABL.

Body of Report

Task 1 (Specific Aim 1) To determine whether the DNA Ligase III/XRCC1/PARP/WRN complex is recruited to in vivo DSB.

Rationale:

We have shown that the DNA Ligase III/XRCC1/WRN "back-up" repair complex is significantly up-regulated in BCR-ABL-positive CML cells and at low levels in controls cell lines. It is however important to show that this complex is involved in the repair of DSB *in vivo*.

WRN and DNA ligase IIIα co-localize with DRneo at ISce-1 induced DSBs

To investigate the role of WRN and DNA ligase IIIα in DSB repair in BCR-ABL positive CML, K562 and control NC10 cells were stably transfected with the DRneo plasmid that contains the ISce-1 restriction site that is not present in the mammalian genome (K562DRneo and NC10DRneo, **Figure 2A**)(Richardson & Jasin 2000). Subsequent transfection of these cells with expression constructs for ISce-1 endonuclease specifically induces a DSB into the genome of these cells (Richardson & Jasin 2000). A combined fluorescence *in situ* hybridization (FISH)-immunostaining technique was used to determine whether DNA ligase IIIα and WRN localize to the ISce-1 induced DSBs (Rassool et al. 2003, Rassool et al. 1996). The efficiency of DSB induction, following transfection of the ISce-1 endonuclease, was determined by the nuclear co-localization of γH2AX, a key marker for DSBs, and the DRneo signal.

Two hundred nuclei were analyzed from each of at least 3 experiments. Approximately 12% percent of K562DRneo (**Figure 2B**) and 8% NC10DRneo cells had induced DSB, as shown by co-localization of γ-H2AX and DRneo. In CML (**Figure 2B**) 8% of cells show co-localization of Ku86 with DRneo vs 6% in NC10 cells, following I-Sce1 expression. In contrast, the co-localization of DNA ligase IV with DRneo (**Figure 2B**) was significantly lower in CML cells (1%), compared with NC10 cells (4%). More strikingly, while we had difficulty detecting co-localization of either DNA ligase IIIα or WRN with DRneo in NC10 cells, DNA ligase IIIα and WRN (**Figure 2B**) did co-localize with DRneo in K562 cells at a frequency of about 2%. Because the antibodies have different affinities for their target protein, it is not possible to compare the co-localization frequencies obtained with different antibodies. Nonetheless, this approach does reveal quantitative differences in the co-localization of a specific protein in different cell lines and, importantly, showed that DNA ligase IIIα and WRN are specifically recruited to DSBs in CML cells, providing evidence that these proteins are participants in the altered DSB repair in these cells.

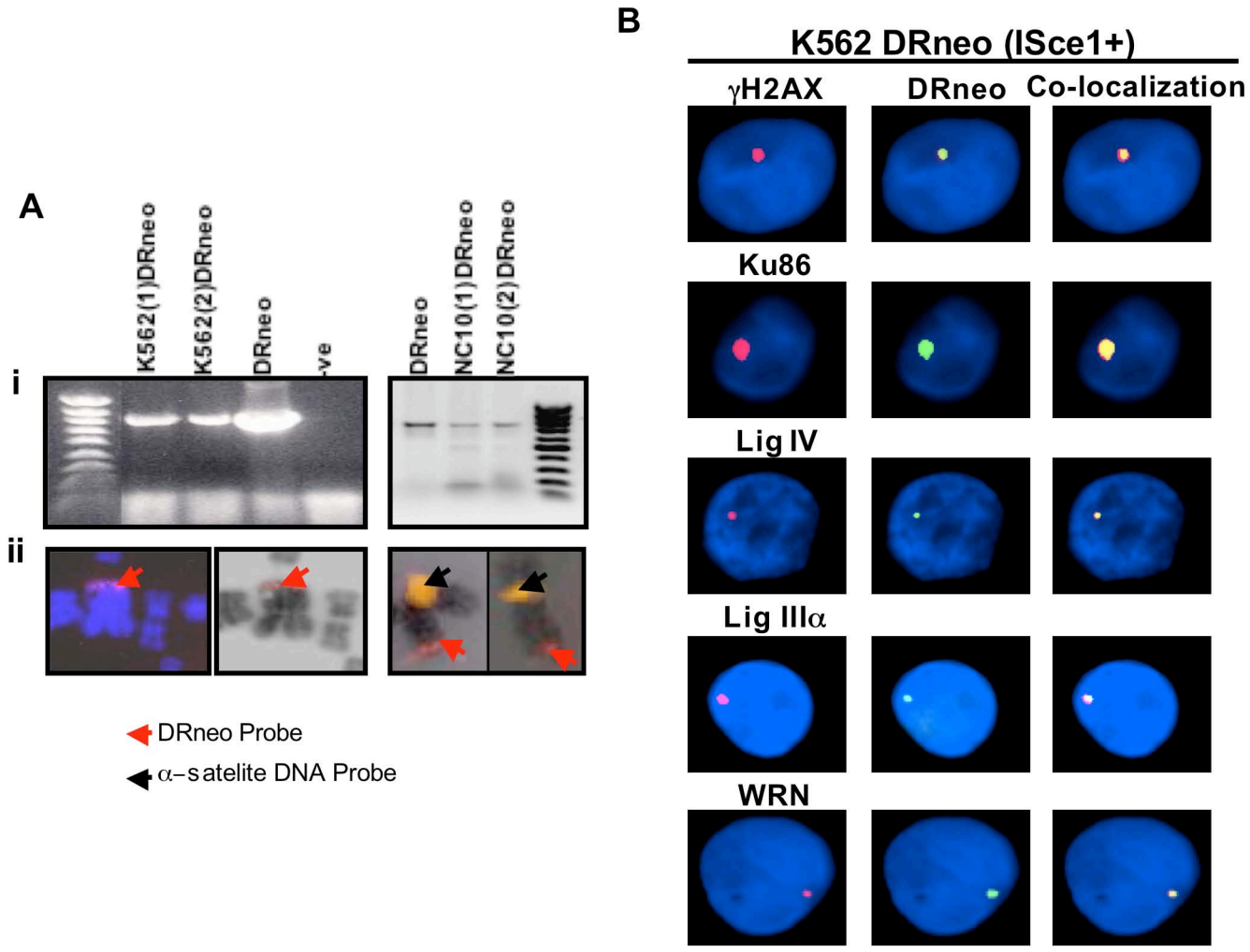

Figure 1 A(i): Detection of integrated DRneo in K562 and NC10 cell clones stably transfected with DRneo (K562DRneo and NC10DRneo, respectively) by PCR. (ii): The DRneo construct labeled with spectrum red was used for FISH analysis of metaphase spreads prepared from K562DRneo cells. The DRneo was integrated at a telomeric position on the chromosomes as shown in DAPI stained (left, red arrow) and G-banded (middle, red arrow) images. Two-color FISH was used to localize DRneo to chromosome 4 in K562DRneo cells (right image). Chromosomes from two different metaphase cells shown with yellow signal indicating chromosome 4 alpha satellite probe, localized to the centromere (black arrow) and red signal localizing the DRneo probe to the telomeric region of the chromosome (red arrow). B: Co-localization of DRneo and γH2AX, Ku86, DNA ligase IV, DNA ligase IIIα, and WRN in K562DRneo cells by FISH. Images show co-localization of DRneo (FITC, green signal) and above mentioned proteins (TRITC, red signal) in K562DRneo cells transfected with ISce-1. Nuclei are stained with DAPI (blue). Right hand panels are merged images of FITC and TRITC showing co-localization.

Task 2 (Specific Aim 2) ***To determine that the fidelity of DSB repair can be altered by modulation of components of the DNA Ligase III/XRCC1/PARP/WRN protein complex and/or Artemis.***

Rationale:
Although we have shown that the Ligase III/XRCC1/PARP/WRN protein complex is peculiar to BCR-ABL positive cells, it is important to determine whether this protein complex plays a role in creating DSB repair infidelity, leading to mutations and deletions.

(A) siRNA down-regulation of WRN and DNA ligase IIIα results in increased DSBs.
In order to demonstrate that WRN and DNA ligase IIIα play a role in repairing DSBs in BCR-ABL positive CML, we examined whether their down-regulation results in an increased level of unrepaired DSB. Following siRNA knockdown of either WRN (approximately 90% reduction at 72 hours) or DNA ligase IIIα (approximately 75% reduction at 72 hours) in CML cells (**Figure 2A**), there was a significant increase ($p<0.01$) in the number of γH2AX foci (**Figure 2B, C**). Together, these results suggest that both WRN and DNA ligase IIIα play a role in repair of endogenously generated DSBs in CML cells.
Next, we examined the role of WRN and DNA ligase IIIα in the repair of DSBs generated by exogenous agents in CML cells. The number of γH2AX foci was determined in K562 cells 6 hours after exposure to 2.5 Gy of γ-radiation. There was a marked defect in the repair of DSBs induced by ionizing radiation in cells with reduced levels of DNA ligase IIIα (**$p<0.01$**; **Figure 2B, C**). In contrast, knockdown of WRN did not result in a significant increase in the number of γH2AX foci (**Figure 2B, C**), compared with non-target controls, but the foci were much larger and were similar to those remaining in DNA ligase IIIα knockdown cells.

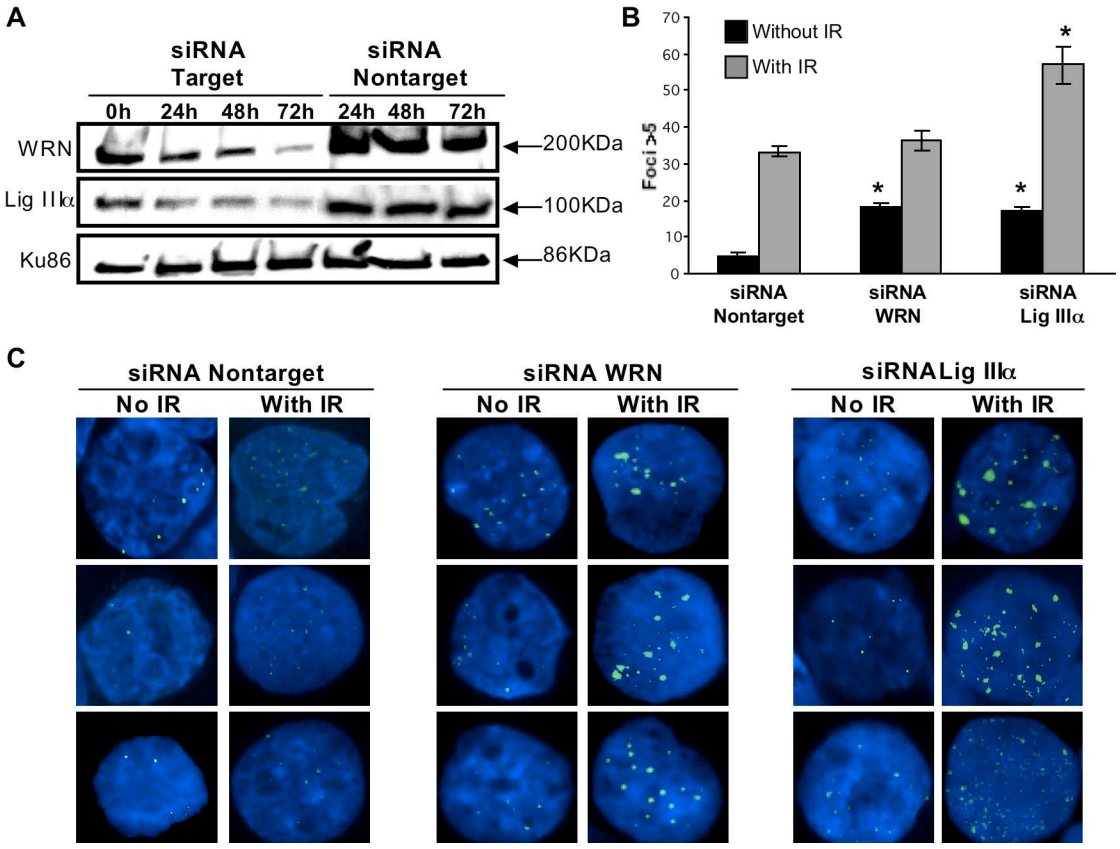

Figure 2 A: Nuclear extracts were prepared at 4 different time points 0h, 24h, 48h and 72h. Western blotting was performed using WRN antibody (90% knockdown; upper panel) and DNA ligase IIIa antibody (75% knockdown; middle panel). siRNA using non-target oligonucleotides were used as controls. Ku86 was used as loading control (lower panel). B. Bar graph showing the percentage of K562 cells with more than 5 gH2AX foci examined in siRNA non-target, siRNA knockdown of WRN and DNA ligase IIIa cells with or without irradiation (IR; 2.5 Gy). Black bars indicate no IR and grey bars are with IR treatment. 200 nuclei were examined from each of 3 different experiments. Values significantly different are marked with an asterisk ($p<0.01$ by Student's t-test). Error bars reflect the standard error of the mean. C. Images of three different cells showing gH2AX foci (FITC, green signal) in K562 following siRNA non-target (left panels), siRNA down-regulation of WRN (middle panels) and DNA ligase IIIa (right panels), with and without irradiation.

(B) Knockdown of DNA ligase IIIα and WRN decreases the end-joining efficiency in CML cells.
To more directly define the role of WRN and DNA ligase IIIα in the repair of DSB in CML, an *in vivo* plasmid end-joining assay was performed. Following knockdown of either WRN or DNA ligase IIIα, a pUC18 plasmid containing a DSB within LacZα was transfected into K562 cells. Circularized (repaired) plasmid DNA was extracted from K562 cells and used to transform E. coli, as previously reported (Gaymes et al. 2002a). Reducing the levels of either DNA ligase IIIα (**Figure 3A**) or WRN (**Figure 4A**) results in a 2-3 fold reduction in the number of colonies, indicating a decrease in end-joining efficiency in the BCR-ABL positive CML cells ($p<0.01$). Analysis of the colonies from the plasmid reactivation assays for their frequency of repair errors, i.e., white (incorrectly repaired) vs total colonies (blue [correctly repair]+ white)(Gaymes et al. 2002a) , revealed that knockdown of DNA ligase IIIα results in a significant increase ($p<0.01$) in the frequency of misrepaired colonies (**Figure 3B**). There was no significant change in the percentage of misrepair events that resulted in large deletions, defined as >20 bp (**Figure 3C, D**). In contrast, knockdown of WRN did not increase the frequency of misrepaired colonies (**Figure 4B**), but there was a significant ($p<0.01$) increase (approximately 3 fold) in the percentage of colonies with large deletions (**Figure 4C, D**).
To determine whether knockdown of either DNA ligase IIIα or WRN leads to differences in repair utilizing DNA sequence microhomologies, we sequenced the breakpoint junctions of 15 repaired plasmids from each of the LacZα reactivation experiments. The majority (80%) of plasmids in K562 cells are repaired utilizing DNA microhomologies of 2 to 6 bp . In contrast, plasmids from cells with reduced levels of either DNA ligase IIIα (25%; $p<0.001$; **Figure 3E**) or WRN (40%; $p<0.001$; **Figure 4E**) had very short or no sequence microhomologies at the breakpoint junctions in repaired plasmids. Finally, we determined that siRNA knockdown of either WRN or DNA ligase IIIα in CML cells results in a small but reproducible decrease in viability as measured by trypan blue exclusion.

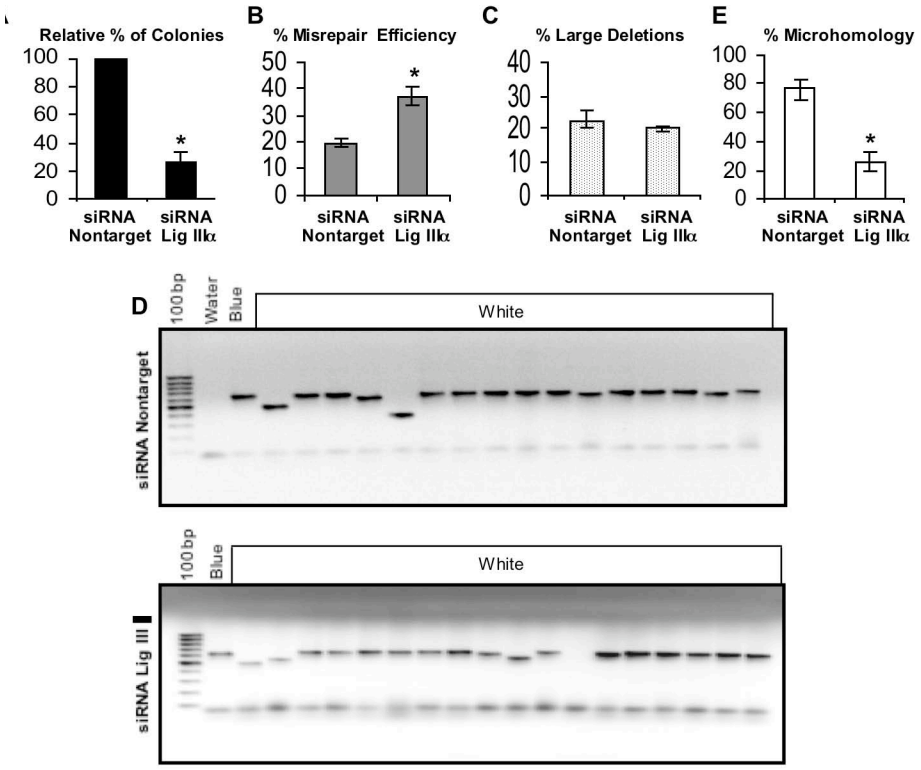

Figure 3 An *in vivo* LacZα plasmid reactivation assay was used to measure end-joining in siRNA DNA ligase IIIα down-regulated cells and compared with that using siRNA controls. A: Relative percentage of colonies, indicating the efficiency of end-joining. B: The percentage of misrepair, i.e. the number of white colonies as a percentage of total colonies (blue+white). C. Graph of percentage large deletions, defined as > 20bp. D. Agarose gel showing PCR products of repaired colonies in siRNA non-target controls and siRNA knockdown of DNA ligase IIIα. E: The percentage of plasmids repaired using DNA sequence microhomologies of 2-6bp. Fifteen plasmids were sequenced Values significantly different are marked with an asterisk by Student's t-test ($p<0.01$ for A and B and $p<0.001$ for E). Error bars reflect the standard error of the mean.

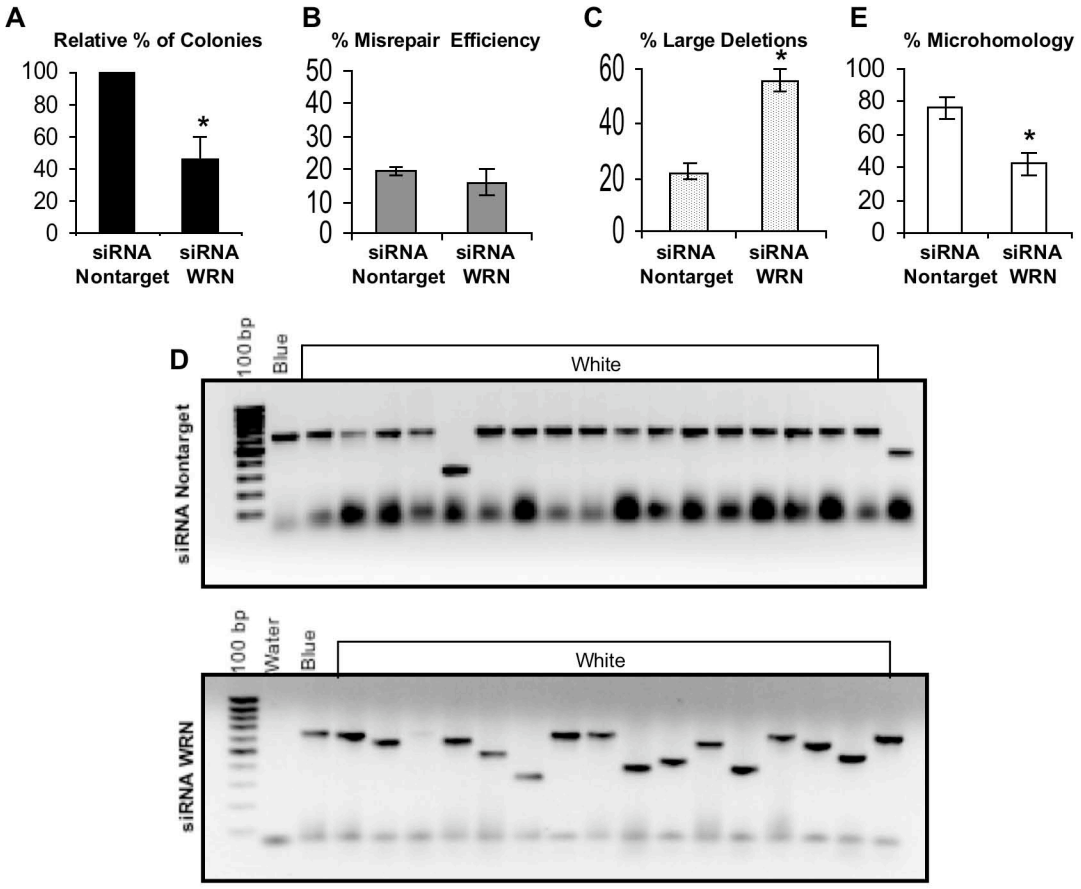

Figure 4. An *in vivo* LacZα plasmid reactivation assay was used to measure end-joining in siRNA down-regulated WRN K562 cells compared with that using siRNA controls. **A**: Relative percentage of colonies indicating the efficiency of end-joining. **B**: The percentage of misrepair, i.e. the percentage of the white colonies as a percentage of total colonies (blue+white). **C.** The percentage of large deletions, defined as > 20bp. **D.** Agarose gel showing PCR products of repaired colonies. **E:** The percentage of plasmids repaired using DNA sequence microhomologies of 2-6bp. Fifteen plasmids were sequenced. Values significantly different are marked with an asterisk by Student's t-test ($p<0.01$ for A and $p<0.001$ for C and E). Error bars reflect the standard error of the mean.

(C) Artemis over-expression leads to a decreased in large deletions

To determine whether the reduced levels of Artemis contribute to the aberrant DSB repair in CML, Artemis was over-expressed in K562 cells (**Figure 5A**). Although Artemis over-expression did not significantly alter the end-joining efficiency (**Figure 5B**), it results in a considerable decrease in the size of DNA deletions at misrepaired DSB **(**p<0.001**; Figure 5C,D).** In addition, analysis of the breakpoint junctions from 15 repaired plasmids in K562 cells overexpressing Artemis show a decrease in repair using DNA sequence microhomologies down to 33%, compared with empty vector controls (80%) (p<0.001**; Figure 5E, Table 1**). Thus, down-regulation of Artemis in CML results in abnormal processing of DSBs.

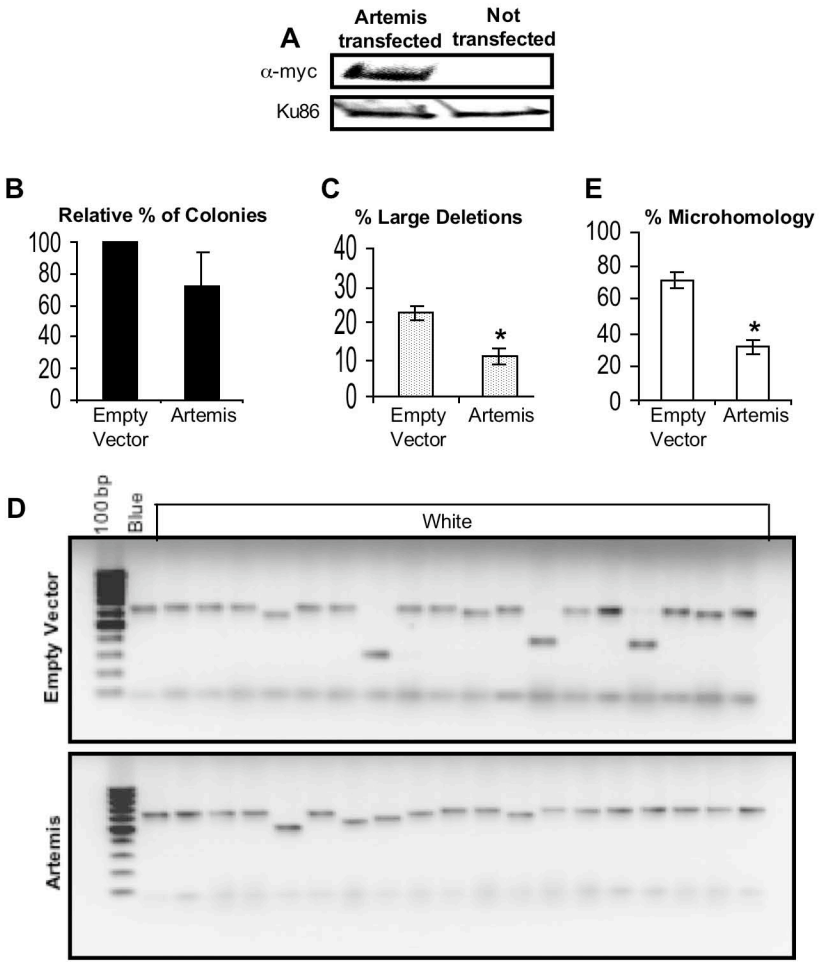

Figure 5 A: Western blotting in K562 cells transfected with the myc-tagged Artemis cDNA construct (pcDNA huASC1D) showing Artemis over-expression. Ku86 was used as loading control. An *in vivo* LacZα plasmid reactivation assay was used to measure end-joining in Artemis over-expressed cells, compared with empty vector transfected controls. **B**: Relative percentage of colonies, indicating the efficiency of end-joining. **C.** Graph of percentage large deletions, defined as > 20bp. **D.** Agarose gel showing PCR products of repaired colonies in empty vector controls and Artemis overexpressed K562 cells. **E:** The percentage of plasmids repaired using DNA sequence microhomologies of 2-6bp. Fifteen plasmids were sequenced. Values significantly different are marked with an asterisk by Student's t-test (p<0.001 for C and E). Error bars reflect the standard error of the mean.

Task 3

(Specific Aim 3) ***To define the relationship between BCR-ABL and the protein complex containing DNA Ligase III, XRCC1, PARP and WRN we will modulate BCR-ABL expression in CML cells and test for formation of the "back-up" complex and repair infidelity.***

Rationale

Our preliminary data showed that the Ligase III and WRN proteins are significantly up regulated in BCR-ABL-positive CML cell lines. It is necessary therefore to determine whether BCR-ABL expression leads to increased levels of "back-up" proteins.

BCR-ABL expression leads to up-regulation of DNA ligase IIIα and WRN.

To determine whether BCR-ABL expression is necessary and sufficient for formation of the "back-up" protein complex, we overexpressed BCR-ABL (plasmid constructs containing BCR-ABL cDNA, kindly donated by Dr Van Etten, Tufts, Boston) in immortalized human myeloid progenitor cells (Mo7E, a kind gift from Dr Takebe, University of Maryland), using nucleofection, according to protocols from AMAXA (www.amaxa.com).
We find that the steady state level of DNA ligase IIIα and WRN is increased in MO7e cells stably expressing BCR-ABL (P210MO7e), compared with isogenic MO7e cells (**Figure 6A**).

To provide additional evidence for the relationship between DNA ligase IIIα and WRN and expression of the BCR-ABL, we examined the levels of these proteins in primary samples (N=4) from patients with different levels of BCR-ABL, following treatment with the tyrosine kinase inhibitor Gleevec. Nuclear extracts from patient cells demonstrate that the steady state levels of WRN and DNA ligase IIIα are reduced in patient sample (CML1) where BCR-ABL levels (60%) are significantly decreased, as assessed by fluorescence in situ hybridization (FISH) (**Figure 6B**). In contrast, the level of the Ku86 subunit does not change significantly (**Figure 6B**). These data, together with that in Figure 5A suggest that the increased steady state levels of DNA ligase IIIα and WRN may either be a direct effect of BCR-ABL or a consequence of the increased levels of ROS and DNA damage caused by BCR-ABL expression.

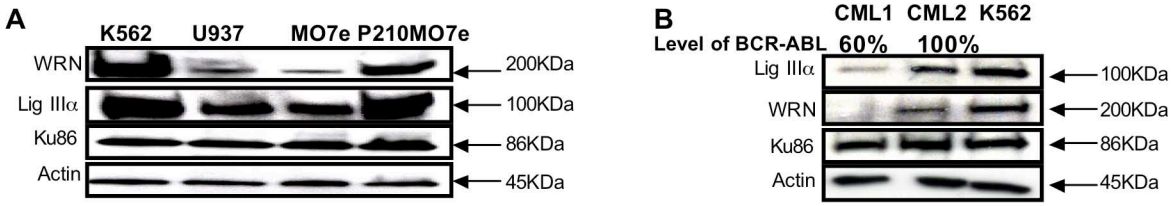

Figure 6 A: BCR-ABL negative MO7e shows down-regulation of DNA ligase IIIα and WRN compared with BCR-ABL positive P210MO7e and K562. Western blotting using nuclear extracts from two BCR-ABL positive cell lines (K562 and P210MO7e) and BCR-ABL negative cell lines (U937 and MO7e). Actin was used as loading control. **B**: Primary CML bone marrow mononuclear cells show down-regulation of DNA ligase IIIα and WRN. Western blotting using nuclear extracts from CML cell line (K562) and two CML patients (CML1 and 2) post Gleevec treatment (6-12 months). Patient CML1 shows decreased DNA ligase IIIα and WRN expression with decreased levels of BCR-ABL positivity by FISH. Patient CML2 shows increase expression of DNA ligase IIIα and WRN, with 100% BCR-ABL positivity. BCR-ABL positive CML cell line K562 was used as a positive control. Ku86 and Actin were used as loading controls.

Work outstanding in Task 3:

To determine the levels of BCR-ABL and "back-up" complex necessary for repair infidelity, we will abrogate BCR-ABL expression in Ph-positive CML cell lines (K562, MEG01, KU; ATCC) by imatinib treatment, according to protocols of Branford and Hughes(Branford & Hughes 2006a, Branford & Hughes 2006b) et al. At time points following imatinib administration (24 to 96 hrs), levels of the BCR-ABL fusion protein will be measured by Western blotting analysis, formation of the back-up protein complex will be measured by immunoprecipitation, and misrepair frequencies will be determined, as we have previously described (Gaymes et al. 2002b).

Key Research Accomplishments:

We report that:

- The **novel "Back-up" repair protein complex,** involving WRN and DNA ligase IIIa, we have identified in CML cells, **localizes to DSB**.

- These proteins repair DSB because their "down-regulation" (a) increases the number of **unrepaired DSB**, and (b) affects the **repair efficiency** in CML cells. Over expression of Artemis, the main NHEJ protein found down regulated in CML cells, increases correct repair of DSB.

- We have preliminary data that expression of "Back-up" repair proteins **is dependent on expression of BCR-ABL**.

Reportable outcomes:

- We have a manuscript in revision in a high impact sub-specialty journal, Blood, describing this work (appendix).

- This work has resulted in presentation of a poster at the American Society of Hematology (appendix)

- This work has been presented in invited talks at 2 international meetings (appendix).

Conclusion:

- The aims of Task 1 have been completed. We find WRN and DNA ligase IIIa co-localize with DRneo at ISce-1 induced DSBs

- The aims of task 2 have been completed. We find that siRNA down-regulation of WRN and DNA ligase IIIα results in increased DSBs and a decreased efficiency of repair.

- The aims of Task 3 have been partially completed, showing that BCR-ABL expression leads to up-regulation of DNA ligase IIIα and WRN.

- Experiments to complete Task 3 involve treatment of BCR-ABL expressing cells with Gleevec followed by Western blotting and Immunoprecipitation for "back-up" proteins. This work will be completed during the period of the grant extension.

- To further confirm that "Back-up" proteins are involved in repair of excess DSB in CML cells, we will use recently developed Ligase inhibitors to test BCR-ABL–positive CML cells for alteration of DSB,

repair and cell survival. This represents an extension of the original statement of work to be completed during the remaining granting period.

- These results will lay the groundwork for future studies to test whether this aberrant protein complex is important in survival of CML cells. Inhibition of these proteins may be a mechanism for killing CML cells.

References

BRADY N, GAYMES TJ, CHEUNG M, MUFTI GJ & RASSOOL FV (2003) Increased error-prone NHEJ activity in myeloid leukemias is associated with DNA damage at sites that recruit key nonhomologous end-joining proteins. Cancer research **63,** 1798-805.

BRANFORD S & HUGHES T (2006a) Detection of BCR-ABL mutations and resistance to imatinib mesylate. Methods Mol Med **125,** 93-106.

BRANFORD S & HUGHES T (2006b) Diagnosis and monitoring of chronic myeloid leukemia by qualitative and quantitative RT-PCR. Methods Mol Med **125,** 69-92.

GAYMES TJ, MUFTI GJ & RASSOOL FV (2002a) Myeloid leukemias have increased activity of the nonhomologous end-joining pathway and concomitant DNA misrepair that is dependent on the Ku70/86 heterodimer. Cancer research **62,** 2791-7.

GAYMES TJ, NORTH PS, BRADY N, HICKSON ID, MUFTI GJ & RASSOOL FV (2002b) Increased error-prone non homologous DNA end-joining--a proposed mechanism of chromosomal instability in Bloom's syndrome. Oncogene **21,** 2525-33.

MELO JV (1996) The molecular biology of chronic myeloid leukaemia. Leukemia **10,** 751-6.

RASSOOL FV, LE BEAU MM, SHEN ML, et al. (1996) Direct cloning of DNA sequences from the common fragile site region at chromosome band 3p14.2. Genomics **35,** 109-17.

RASSOOL FV, NORTH PS, MUFTI GJ & HICKSON ID (2003) Constitutive DNA damage is linked to DNA replication abnormalities in Bloom's syndrome cells. Oncogene **22,** 8749-57.

RICHARDSON C & JASIN M (2000) Coupled homologous and nonhomologous repair of a double-strand break preserves genomic integrity in mammalian cells. Molecular and cellular biology **20,** 9068-75.

SATTLER M, VERMA S, SHRIKHANDE G, et al. (2000) The BCR/ABL tyrosine kinase induces production of reactive oxygen species in hematopoietic cells. The Journal of biological chemistry **275,** 24273-8.

Appendices

1. Abstract American society of Hematology. December 8-11 (2007)

Up-regulated WRN and DNA Ligase IIIa are involved in Alternative NHEJ Repair Pathway of Double Strand Breaks (DSB) in Chronic Myeloid Leukemia (CML)

Annahita Sallmyr and Feyruz Rassool

2. Invited talks at National/International Meeting

European Society of Hematology: Chronic mueloid leukemia workshop

Global Workshop on Myeloproliferative Diseases

3. Full Manuscript (in revision in Blood)

Title: Up-regulation of WRN and DNA ligase IIIa in Chronic Myeloid Leukemia: Consequences for the repair of DNA Double Strand Breaks

Annahita Sallmyr, Alan E. Tomkinson, and Feyruz V. Rassool

1. Abstract

[1016] Up-Regulated WRN and DNA Ligase III Are Involved in Alternative NHEJ Repair Pathway of DNA Double Strand Breaks (DSB) in Chronic Myeloid Leukemia (CML). Session Type: Poster Session, Board #170-I

Annahita Sallmyr, Feyruz V. Rassool Radiation Oncology, University of Maryland School of Medicine, Baltimore, MD, USA

The oncogenic BCR-ABL in CML produces increased reactive oxygen species (ROS) leading to DSB and aberrant repair. We have previously shown that CML cells demonstrate an increased frequency of errors of non homologous end-joining (NHEJ). DSB are repaired by two major pathways, homologous recombination (HR) and NHEJ, the dominant pathway in eukaryotic cells, also known as DNA-PK dependent NHEJ (D-NHEJ). Recent reports have identified alternative or back-up NHEJ pathways (B-NHEJ) that are highly error-prone, and may explain the altered DSB repair reported in CML. To determine the mechanism for the aberrant NHEJ repair in CML, we examined steady state levels of D-NHEJ proteins, including Ku70/86, DNA-PKcs, Artemis and DNA Ligase IV/XRCC4 in four different BCR-ABL positive CML cell lines compared with three lymphoblastoid cell lines established from normal individuals and one BCR-ABL negative CML cell line. We find that two key components of D-NHEJ, Artemis (4-7 fold) and DNA Ligase IV (2-3 fold) are down-regulated, compared with controls. These data suggest that D-NHEJ repair is compromised in CML. To determine whether alternative NHEJ repair plays a role in the aberrant repair of DSB in CML cells, we next examined expression levels of DNA Ligase III/XRCC1, PARP and other proteins known to be associated with NHEJ repair, such as the protein found to be deleted in Werners syndrome, WRN. We find that WRN and DNA Ligase III are increased (3-6 fold) in BCR-ABL-positive CML compared with control cell lines. Importantly, DNA Ligase III/XRCC1 forms a complex with WRN, suggesting that it may be a new member of the alternative repair pathway. To confirm that up-regulation of DNA Ligase III and WRN are elicited by BCR-ABL, we examined the levels of these proteins in primary samples (N=4) from patients with different levels of BCR-ABL, following treatment with the tyrosine kinase inhibitor Gleevec. WRN and DNA Ligase III are down regulated in patient samples where BCR-ABL levels are significantly decreased. Furthermore, we confirmed that these up-regulated proteins are involved in DSB repair in CML cells because they co-localize to induced DSB in BCR-ABL-positive cell lines stably transfected with DSB-containing DRneo plasmid, using fluorescence in situ hybridization (FISH) co-immunostaining. Importantly we show that siRNA down-regulation of WRN and DNA Ligase III leads to elevated levels of unrepaired DSB and a decreased frequency of DSB repair efficiency in CML cells. In addition siRNA down-regulation of WRN leads to large deletions at the site of repair, while siRNA down-regulation of DNA Ligase III results in an increased frequency of misrepair. Finally, we determined whether correction of main NHEJ pathway proteins in CML can lead to a decrease in the frequency of errors of end-joining repair. Over-expression of Artemis using pcDNA constructs in CML cells leads to more correct end-joining, compared with vector transfected controls. We conclude that down-regulation of Artemis and DNA Ligase IV leads to compensatory up-regulation of alternative repair pathways in BCR-ABL-positive CML cells, and suggest a role for a new protein complex in CML, in protecting and joining DNA ends, thus ensuring the survival of CML cells. Inhibition of alternative NHEJ repair may be explored in combination with other agents as a therapeutic strategy in CML.
Abstract #1016 appears in Blood, Volume 110, issue 11, November 16, 2007
Keywords: Chronic Myeloid Leukemia|DNA Repair|Genomic Instability
Disclosure: No relevant conflicts of interest to declare.

Saturday, December 8, 2007 5:30 PM

Session Info: Poster Session: Chronic Myeloid Leukemia: Biology and Pathophysiology I (5:30 p.m.-7:30 p.m.)

2. Invited Talks

CML Workshop in September 07, Mandelieu France

Title of Talk : Error-prone Repair of DSB by "Back-Up" Non-homologous end-joining: a Model for Creating Genomic Instability in CML?

Program

EUROPEAN SCHOOL OF HAEMATOLOGY

CML – Prospects for the 21st century

Mandelieu, France, 27-30 September 2007

Organisers: Angelo M. Carella, Jorge Cortes, George Daley, John M. Goldman, Francois Guilhot, Rüdiger Hehlmann, Junia V. Melo, Giuseppe Saglio

DRAFT PROGRAM 31-07-07

Friday, 28 September

08.30 – 08.35 Welcome John Goldman and Angelo Carella

08.35 – 10.30 Session 1 Basic studies / Mechanisms

Chair: Alan Gewirtz

Keynote: O Hantschel (Vienna) (20)
The Bcr-Abl molecular machine as the target for imatinib/dasatinib/nilotinib

NCP Cross (Salisbury) (10)
New recurrent abnormalities in BCR-ABL negative CML

C Eaves (Vancouver) (10)
Unique features of chronic phase CML stem cells

T Holyoake (Glasgow) (10)
Inducing apoptosis of CML stem cells

F Frassoni (Genoa) (10)
Impact of imatinib on leukemic stem cell burden in CML patients

A Turhan (Poitiers) (10)
STAT3 activation in CML

Discussion

11.00- 13.00 **Session 2** **Animal Models**

Chair: Barney Clarkson

Keynote: R van Etten (Boston) (20)
Targeting the survival and engraftment of CML stem cells

E Passegue (San Francisco) (10)
Understanding JunB function in hematopoietic stem cell maintenance and leukemic stem cell generation

D Cilloni (Torino) (10)
BCR-ABL transgenic drosophila

Session 3 **Basis of Genomic Instability**

Chair: Giuseppe Saglio

Keynote: T Skorski (Philadelphia) (20)
BCR/ABL kinase induces DNA damage and impairs DNA repair, cell cycle checkpoints, and apoptosis, leading to genomic instability

F Rassool (Baltimore) (10)
Error-prone repair of double strand breaks by "back-up" non homologous end-joining (NHEJ): a model for creating genomic instability in CML?

Panel Discussion (1)
N von Bubnoff, S Kamel-Reid, J Kuroda, G Rosti, C Preudhomme

14.00 – 16.30 **Session 4** **Profiling, progression, BCR-ABL effectors**

Chair: Pierre Laneuville

X Jiang (Vancouver) (10)
AHI-1, a novel signaling protein, interacts with BCR-ABL and modulates BCR-ABL transforming activity and imatinib sensitivity of primitive CML cells

P Vigneri (Catania) (10)
BCR-ABL modifies the expression and function of the IRF-5 transcription factor

JV Melo (London) (10)
Biomarkers for prognosis in CML

J Radich (Seattle) (10)
Regulation of progression and response

J Duyster (Munich) (10)
Retroviral insertional mutagenesis for identification of genes contributing to persistence of CML cells

D Perrotti (Columbus) (10)
Molecular defects responsible for progression of CML: targeting phosphatases as new and alternative

therapeutic approach for imatinib/dasatinib- sensitive and -resistant Ph-positive leukemias

C Gambacorti-Passerini (Monza) (10)
Beta-catenin and Bcr/Abl: a dangerous liaison

T Brümmendorf (Hamburg) (10)
Identification of novel targets for BCR-ABL by proteomics

Discussion

17.00 - 18.30 **Session 5** **Imatinib updated (molecular, clinical toxicity)**

Chair: Steve O'Brien

Keynote: C Schiffer (Detroit) (20)
TKIs: What problems remain?

F Guilhot (Poitiers) (10)
Does imatinib really increase survival of patients in previously untreated chronic phase:
a comprehensive review of large phase III trials

M Molimard (Bordeaux) (10)
Through plasma imatinib concentrations are associated with responses to imatinib in CML and improve the standard management

A Quintas-Cardama (Houston) (10)
High dose imatinib - still an option?

J Reiffers (Bordeaux) 10)
Dose escalation for CML-CP patients with suboptimal response or resistance to imatinib

A Reiter (Mannheim) (10)
Tyrosine kinase inhibition in eosinophilia-associated myeloproliferative disorders

F-X Mahon (Bordeaux) (10)
Imatinib mesylate discontinuation in patients with CML in complete molecular remission: an update

Panel Discussion (2) – What are the challenges today?
J Kaeda, L Foroni, E Jabbour, Ph Rousselot, JJ Cornelissen

Saturday, 29 September

08.00–10.00 **Session 6** **Mechanisms of resistance**

Chair: **Junia Melo**

Keynote: M. Deininger (Portland) (20)
Combinatorial kinase inhibitor strategies to eliminate mutation-based drug resistance in BCR-ABL-positive leukemia

M Azam (Boston) (10)
Role of the gatekeeper mutations in kinase activation and drug resistance

S Soverini (Bologna) (10)
Resistance to tyrosine kinase inhibitors: mutations ... and more?

G Martinelli (Bologna) (10)
New mechanisms of resistance in Ph+ leukemia and new drugs to overcome it

Discussion

10.30 – 12.30 Session 7 How to predict response to imatinib and then monitor patients?

Chair: Richard Stone

Keynote: T Hughes (Adelaide) (20)
Predictive tests for imatinib response

RE Clark (Liverpool) (10)
Drug transporters as a critical determinant of the efficacy of imatinib and other TKI

G Saglio (Torino) (10)
Molecular monitoring of CML patients undergoing imatinib therapy: evidence and shadows

JJWM Janssen (Amsterdam) (10)
Immunophenotyping to distinguish Ph+ and Ph- stem cells

JM Goldman (London) (10)
Interpreting transcript levels

Panel Discussion (3) - What issues are still important?
F Cervantes, D Marin, T Mughal, G Ossenkoppele, B Simonsson, JL Steegmann, J Tanzer

14.00 - 16.00 Session 8 - Second generation tyrosine kinase inhibitors

Chair: Rüdiger Hehlmann

Keynote: N Shah (Los Angeles) (20)
Improving molecular treatment using dasatinib as a single agent or in combination TKI therapy

J Cortes (Houston) (10)
Nilotinib

S Kimura (Kyoto) (10)
INNO-406, a Bcr-Abl/Lyn inhibitor from bench to clinic

J Cortes (Houston) (10)
Bosutinib (SKI-606): the new kid on the block

F Cervantes (Barcelona) (10)
Complications associated with newer TKIs

A Quintas Cardama (Houston) (10)
Next generation agents for resistant CML, including MK-0457

F Nicolini (Lyon) (10)

TKI plus chemotherapy for blastic phase CML and Ph-positive acute leukemia

Discussion

16.30–18.30 Session 9 Immunological aspects of stem cell transplantation

Chair: Alois Gratwohl

A Fefer (Seattle) (10)
Syngeneic BMT for CML in chronic phase: an update of the Seattle data

JF Apperley (London) (10)
Syngeneic transplants – EBMT data

C Crawley (Cambridge, UK) (10)
Reduced intensity or myeloablative transplants?

AM Carella (Genoa) (10)
RIC SCT for older patients

A Devergie (Paris) (10)
Treating CML in relapse after allo-SCT with imatinib

Panel Discussion: SCT in 2007 (40)

Opening presentation: A Gratwohl (Basel) (10)
Risk adapted strategies for SCT

Panel members:
A Gratwohl, R Hehlmann, F Guilhot, J Apperley, C Crawley, AM Carella, JM Goldman

Conference Gala Dinner

Sunday 30 September

8.30-10.00 Session 10 - Immune targets for CML

Chair: Richard Clark

Keynote : F Dazzi (London) (20)
Exploiting GvL without transplant

D Smith (Baltimore) (10)
Vaccination with K562/GM-CSF

M Bocchia (Sienna) (10)
Bcr-Abl peptide vaccination - an update

K Rezvani (London) (10)
WT1/Pr3 peptide vaccination for leukemia

Panel Discussion

F Dazzi, M Bocchia, RE Clark, G Saglio, D Smith, K Rezvani, others

10.00- 10.30 Coffee

10.30 – 11.45 Session 11 - Future initiatives

Chair: John Goldman

M Baccarani (Bologna) (15)
Defining response and failure - 2007

NCP Cross (Salisbury) (15)
Standardization of RQ-PCR

SG O'Brien (Newcastle) (15)
Future of prospective clinical studies

R Hehlmann (Mannheim) (15)
Leukemia-Net – Prospects for the next 5 years

11.45 – 12.00 Concluding remarks

12.00 End of meeting

Myeloproliferative Disease Workshop in December 07, San Juan Puerto Rico

Title of Talk: Understanding Genomic Instability in CML

Agenda

Wednesday, December 12, 2007

8:00 am	Registration and Continental Breakfast	
8:50 am	Welcome and Introductions	John Goldman, Tony Green Tariq Mughal
Session 1	9:00-10:40 am	*Moderator: Tony Green*
	The "Fialkow" Hypothesis	John Goldman
	Is BCR-ABL the Originating Event in CML?	George Daley
	Genetic Complexity of PV, ET, and PMF: Is JAK2V617F the Whole Story?	Ross Levine
	Are CML Stem Cells Genetically Unstable?	Tomasz Skorski
	Epigenetic Regulation in MPDs	Alessandro Vannucchi
	Break	
Session 2	11:10-1:10 pm	*Moderator: George Daley*
	MPDs and CML: Variations on a Theme?	Tony Green
	Atypical MPDs: Novel Genetic Abnormalities	Nick Cross
	KD Mutations at the Stem Cell Level or Only Later?	Simona Soverini
	Progression and Response in CML	Jerald Radich
	Normal and CML Stem Cells	Susan Graham
	Lunch	

Agenda (continued)

Wednesday, December 12, 2007

Session 3	2:00-3:40 pm	*Moderator: Richard Van Etten*
	What Comes Before JAK2?	Radek Skoda
	Understanding Genomic Instability in CML	Feyruz Rassool
	Micro RNAs Act as Decoy Molecules to Restore Granulocytic Maturation of Differentiation-Arrested BCR/ABL+ Myeloid Precursors	Danilo Perrotti
	Modulation of MPD Phenotype by Variable Expression of NF-E2	Heike Pahl
	TBD	Nikolas von Bubnoff
	Break	
Session 4	4:10-5:30 pm	*Moderator: Radek Skoda*
	Phenotype and Genotype in the MPDs	Jerry Spivak
	JAK2 and Stem Cell Fate Decisions	Catriona Jamieson
	Micro-array Findings in CML	Agnes Yong
	Genomic Instability in the Context of the Chromosomal Theory	Rüdiger Hehlmann
	Leucocytosis and Prognosis	Tiziano Barbui
Session 5	5:30-6:30 pm	Moderator: John Goldman
	JAK2: Molecular Mechanisms	William Vainchenker
	Recent Insights Into Targeting CML Stem Cells	Richard Van Etten
	Adjourn	

Agenda

Thursday, December 13, 2007

7:30 am	Continental Breakfast	
Session 5B	**8:00-9:40 am**	***Moderator: John Goldman***
	Why CML Stem Cells are Spared by TKI Pre-clinical Data	Giuseppe Saglio Jean Luc Villeval
Session 6	**9:40-10:20 am**	***Moderator: William Vainchenker***
	Specificity and Mechanism-of-Action of TKIs	Oliver Hantschel
	FIP1L1-PDGFRA in HES and CEL	Jan Cools
	"MPD Stem Cells"	Ronald Hoffman
	Evaluation of the JAK2 Burden	Richard Silver
	Break	
Session 7	**10:35-12:05 pm**	***Moderator: Timothy Hughes***
	Is Preteasome Inhibition Valuable for Myelofibrosis?	Giovanni Barosi
	Dasatinib Highlights	Claude Nicaise/Ted Szatrowski
	Strategies for Cure	Sergio Giralt
	MKO457 in MPDs	Jonathan Harris
	SGX and Beyond	Paul Manley
	Nilotinib Highlights	Richard Woodman
	Predictive Tests for Imatinib Response	Timothy Hughes
	siRNA and micro-RNA in CML	Alan Gewirtz
	Circumventing Clinical Resistance to TKI	Pierre Laneuville
Session 8	**What Questions Have We Really Answered?**	**Tony Green, John Goldman,**

12:05- 1:00 pm	Tariq Mughal, & All Moderators

Adjourn and Lunch

Up-regulation of WRN and DNA ligase IIIα in Chronic Myeloid Leukemia: Consequences for the repair of DNA Double Strand Breaks.

Annahita Sallmyr, Alan E. Tomkinson, and Feyruz V. Rassool*

Department of Radiation Oncology and Greenebaum Cancer Center, University of Maryland School of Medicine, Baltimore, MD 21201.

* To whom correspondence should be addressed.

Feyruz Rassool, Ph.D

University of Maryland School of Medicine

655 West Baltimore Street

BRB 7-023

Baltimore, MD 21201

Phone: 410-706-5337

Fax: 410-706-6666

E-mail: frassool@som.umaryland.edu

Running title: Up-regulation of alternative NHEJ pathways in CML

Total text word count: 5000

Abstract word count: 199

Expression of oncogenic BCR-ABL in CML results in increased reactive oxygen species (ROS) that in turn cause increased DNA damage, including DNA double strand breaks (DSBs). We have previously shown increased error-prone repair of DSBs by non homologous end-joining (NHEJ), in CML cells. Recent reports have identified alternative NHEJ pathways that are highly error-prone prompting us to examine the role of the alternative NHEJ pathways in BCR-ABL-positive CML. Importantly, we show that key proteins in the major NHEJ pathway, Artemis and DNA ligase IV, are down-regulated whereas DNA ligase IIIα, and the protein deleted in Werner's syndrome, WRN, are up-regulated. DNA ligase IIIα and WRN form a novel complex that is recruited to DSBs in CML cells. Furthermore, "knockdown" of either DNA ligase IIIα or WRN leads to increased accumulation of unrepaired DSB, demonstrating that they contribute to the repair of DSBs repair. These results indicate that altered DSB repair in CML cells is caused by the increased activity of an alternative NHEJ repair pathway, involving DNA ligase IIIα and WRN. We suggest that, while the repair of ROS-induced DSBs by this pathway contributes to the survival of CML cells, the resultant genomic instability drives disease progression.

Introduction

In the majority of patients with CML, fusion of parts of the BCR and ABL genes generates the BCR-ABL tyrosine kinase [1]. This fusion protein interacts with a large number of signaling pathways that allow cells to proliferate in the absence of growth factors and protects them from apoptosis in the absence of external survival factors. In addition, this abnormal signaling leads to defective adherence to the extracellular matrix, and promotes survival and metastasis [2].

In addition to, or concomitant with the roles of BCR-ABL noted above, there is emerging evidence that BCR-ABL expression initiates a cycle of genomic instability that has the potential to create other mutations [3]. Specifically, the BCR-ABL kinase induces production of ROS that causes DNA damage, including DSB in CML cells [4-6]. Thus, cells transformed by BCR-ABL, primary CML cells and cell lines established from CML patients have increased endogenous DNA damage as measured by various DNA damage assays [7,8,9]. Mutations and large deletions in CML cells result from aberrant repair of DSB by homologous recombination (HR) and non homologous end-joining (NHEJ), the two major DSB pathways in mammalian cells [6,9,10]. In particular, we have shown that CML cells respond to increasing DNA damage with enhanced DNA repair processes, including an error-prone version of NHEJ that is characterized by a high frequency of large deletions, compared with normal CD34+ve hematopoietic progenitor cells [9,10].

The major NHEJ pathway in human cells is initiated by binding of the Ku70/86 heterodimer to DSB, followed by the recruitment of DNA-dependent protein kinase catalytic subunit (DNA-PKcs) to form the active DNA dependent protein kinase (DNA PK) [11-13]. In addition to its essential kinase activity, DNA PKcs is the end-bridging factor responsible for synapsis of DNA ends. After protein-mediated end-bridging, the DNA ends are subsequently ligated by DNA ligase IV in conjunction with XRCC4 [14]. The majority of DSB generated by agents such as, ROS and X-radiation produce DSB that

rarely have ligatable 5'P and 3'-OH termini. Therefore, the synapsed DNA ends must be processed prior to ligation by DNA ligase IV and XRCC4 during NHEJ. Many of these processing events involve a nuclease because repair by NHEJ frequently results in small DNA deletions (up to approximately 20bp), resulting from resection of the DNA ends back to regions of DNA sequence microhomology [15,16]. There appears to be a redundancy in the nucleolytic processing step because the Artemis nuclease which is phosphorylated and activated by DNA PK is only required for processing a subset of "complex" DNA ends. [17].

Another candidate nuclease is the WRN protein, which is mutated and deleted in the premature aging syndrome, Werner's [18,19]. WRN interacts with DNA-PKcs and the Ku70/86 heterodimer [20-23]. Notably, Li and Comai showed that binding of WRN to Ku86 increases its exonuclease activity [22,23]. Although WRN is a nuclease, WS cells lacking WRN expression, generate extensive deletions when joining linear plasmids by NHEJ, and exhibit chromosomal instability, in particular deletions[24]. This, suggests that while WRN may be participate in the limited nucleolytic processing chracteristic of NHEJ, DNA ends may be exposed to degradation by an as yet unidentified nuclease in the absence of WRN.

Recently, other DNA repair proteins have been identified that can substitute for major NHEJ proteins when they are deficient or down-regulated. This "back-up" repair appears to be slow, inefficient and characterized by an increased frequency of errors generated through microhomology mediated ligation of DNA ends [25-28]. In cells with reduced DNA ligase IV activity, DNA ligase IIIα, which usually functions in single-strand break repair (SSB) and base excision repair (BER) [29], was shown to participate in DSB repair [25]. In cells deficient in the Ku heterodimer, poly (ADP- ribose) polymerase (PARP), an abundant DNA binding protein that normally initiates the repair of ss breaks, was shown to play a role in repair of DSB by NHEJ [25,30-32].

Although the major NHEJ pathway is considered error-prone, the increased frequency and type of repair errors at DSB in CML suggested altered NHEJ repair activity. Therefore, we have examined the steady state expression levels of NHEJ and candidate "back-up" repair proteins. Notably, two proteins from the major NHEJ pathway, Artemis and DNA ligase IV, are down-regulated. In contrast, DNA ligase IIIα which has been implicated in backup NHEJ and WRN are up-regulated and associate in a novel complex in BCR-ABL positive CML cells. Our data suggest that genomic instability in these cells arises because of the reduced activity of the major NHEJ pathway and the increased activity of an error-prone back-up NHEJ pathway involving DNA ligase IIIα and WRN.

Materials and Methods

Cell lines and antibodies

K562, MEG01, KU812 and Kasumi4 are BCR-ABL positive CML cell lines, and BCR-ABL negative cell line U937 (ATCC). MO7e, a BCR-ABL negative human myeloid leukemia and MO7e BCR-ABL (P210MO7e), stably expressing BCR-ABL, a kind gift of Dr Van Etten (Tufts, Boston). NC3, NC10 and NC108 are human lymphoblastoid lines established from normal lymphocytes, a kind gift from Dr Gazdar (UT Southwestern, Tx).

Cell lines were cultured in RPMI (Cellgro) with 2mM L-glutamine (Cellgro) and antibiotics, Penicillin-Streptomycin (GIBCO) supplemented with fetal bovine serum (FBS ATCC), as indicated by the ATCC. Cells were incubated at 37^{o}C in 5% CO_2 in air atmosphere.

Antibodies:

Ku86 (CALBIOCHEM), mouse monoclonal to human Ku86 dilution 1:1000. DNA-PKcs (C-19) (Santa Cruz), goat polyclonal to C-terminal of human DNA-PKcs, dilution 1:500. Artemis (Abcam), goat polyclonal to Artemis, dilution 1:1000. DNA ligase IV (Acris), rabbit polyclonal antibody to human

DNA ligase IV, dilution 1:1000. XRCC4 (Gene Tex. Inc.), mouse polyclonal to human XRCC4, dilution 1:1000. DNA ligase IIIα (Gene Tex, Inc., USA), mouse monoclonal to human DNA ligase IIIα, dilution 1:1000. XRCC1 (Gene Tex, Inc.), rabbit polyclonal antiserum to human XRCC1, dilution 1:5000. WRN (Abcam), rabbit polyclonal to Werner's Syndrome helicase WRN, dilution 1:500. PARP (BD Pharmingen^{TM}), mouse monoclonal to human Poly (ADP-ribose) polymerase1 (PARP1) dilution 1:1000. Anti myc (Invitrogen) dilution 1:1000. Actin (Abcam), mouse monoclonal to beta Actin, dilution 1:5000. HRP rabbit anti goat IgG (CHEMICON). HRP donkey anti goat IgG (Promega). HRP goat anti rabbit (sc-2004). HRP goat anti mouse (BioRad). Anti-Phospho-Histone H2AX (Upstate). Anti mouse IgG FITC conjugate (SIGMA). Anti mouse IgG TRITC conjugate (SIGMA).

Western Blotting

Nuclear extracts were prepared using CelLytic NuClear Extraction Kit (N-XTRACT) using a non-detergent protocol. Cells were lysed in 1x hypotonic lysis buffer from a 10x lysis buffer stock, containing 100 mM HEPES, pH 7.9, 15 mM $MgCl_2$, 100 mM KCl in the presence of 0.1 M DTT and protease inhibitor cocktail containing 4-(2-Aminoethyl) benzenesulfonyl fluoride (AEBSF), Pepstatin A, Bestatin, Leupeptin, Aprotinin and trans-Epoxysuccinyl-L-leucyl-amido (4-guanidino)-butane (E-64). After centrifugation of the disrupted cells in suspension for 20 minutes at 10,000-11,000x g, the supernatant (cytoplasmic extract) were transferred to a fresh tube. For nuclear extract crude nuclear pellets were re-suspended in1x extraction buffer containing 20 mM HEPES, pH 7.9, 1.5 mM $MgCl_2$, 0.42 M NaCl, 0.2 mM EDTA, 25% (v/v) Glycerol. To 147 µl of 1x extraction buffer, 1.5 µl of the prepared 0.1 M DTT solution and 1.5 µl of the protease inhibitor cocktail were added, shaked gently for 30 minutes and centrifuged for 5 minutes at 20,000-21,000x g. The supernatant were transferred to a clean, chilled tube, snap-froze in aliquots with liquid nitrogen and stored at -70^{o}C. Nuclear extract (50 µg) was boiled in 2x Laemmli sample buffer (BIO-RAD) for 10 minutes. The proteins were separated

on either 7.5% or 4-15% SDS-PAGE and transferred on PVDF membrane. After blocking, membranes were probed with first antibody and secondary antibody as indicated above. ECL (Amersham Biosciences) was used for detection of the proteins.

Immunoprecipitation

Protein A agarose (Upstate) was washed twice with PBS and restored to a 50% slurry with PBS. The nuclear lysate (1 mg/ml), using CelLytic NuClear Extraction Kit (N-XTRACT) as mentioned above was pre-cleared adding 100 µl protein A bead slurry per 1 mg of cell lysate and incubating at 4^{o}C for 10 minutes. Protein A beads were removed by centrifugation at 14,000 rpm at 4^{o}C for 5 seconds. The supernatant was transferred to a fresh centrifuge tube. WRN or DNA ligase IIIα antibodies were added to cell lysate and gently mixed for 2 hours at 4^{o}C on a rocker. The immunocomplex was captured by adding 100 µl protein A beads slurry and gently rocking overnight at 4^{o}C. The agarose beads were collected by pulse centrifugation 5 seconds at 14,000 rpm. The supernatant fraction was discarded and the beads were washed 3 times with 1 ml of ice-cold PBS. The agarose beads were resuspended in 60 µl 2x laemmli sample buffer, mixed gently and boiled for 5 minutes to dissociate the immunocomplex from the beads. The beads were collected by centrifugation and SDS-PAGE was performed with the supernatant fraction.

K562 and NC10 DRneo transfectants

K562 and NC10 cells were stably transfected with DRneo plasmid in the presence of 350 µg/ml hygromycin B (Cellgro). Stable K562 and NC10 containing DRneo plasmid engineered with an inducible DSB, ISce-1 [33]. DSB were induced in stable transfectants by transient transfection of the unique ISce-1 restriction enzyme construct (1 µg /1x10^{6} cells) using Amaxa nucleofector kit V. Following induction of the ISce-1 DSB, fluorescence in situ hybridization (FISH) co-immunostaining was performed as previously described [34] to co-localize γH2AX, Ku86, DNA ligase IV, DNA ligase IIIα

and WRN proteins to the ISce-1 site of DRneo. Briefly, DRneo labeled with biotin and detected with FITC-conjugated avidin (green signal). Thereafter, cells were immunostained for these proteins and detected indirectly with TRITC-conjugated IgG.

Fluorescence in situ hybridization (FISH)

FISH was performed as previously described [34]. Probes were prepared by nick-translation using Bio-11-dUTP (Enzo Diagnostics), digoxygenin-11-dUTP (Boehringer Mannheim), or with directly labelled nucleotides (Gibco-BRL or Vysis). The hybridization mixture contained the labeled DRneo probe (5.0-10 μg/ml), competitor DNA (unlabeled, sonicated, total human genomic DNA, 0.05-0.1 mg/ml), and the Cot1 fraction of DNA (0.05-0.1 mg/ml). Probes were hybridized to cytospin preparations of cells overnight at 37^{o}C in a humidity chamber, and subsequently slides were washed according to standard protocols. Slides were pre-incubated in blocking buffer (4XSSC containing 2% bovine serum albumin (BSA) and 0.2% triton X) for 30 minutes, and then incubated for up to 1 hour with FITC-conjugated antibody. After washing and blocking, slides were incubated for 1 hour with primary antibody diluted in blocking buffer at 37^{o}C in a humidity chamber. Slides were then washed three times for 4 minutes each in 4XSSC containing 2% Tween 20 and incubated with secondary antibody conjugated to TRTC fluorochrome. Secondary antibodies (Sigma) were used at 1:100 dilution. Interphase nuclei were counter-stained with 4,6 diamino-2-phenylindole-dihydrochloride (DAPI).

Immunocytochemistry

Cells were harvested and washed in PBS and centrifuges at 800-1000x g for 5 minutes. Cells were cytospined and fixed in 2% paraformaldehyde (P-6148, from SIGMA) for 10 minutes at room temperature and washed 3x 3 minutes. Cells were permeabilized in a Triton X-100 solution for 5 minutes at room temperature. The slides were blocked in a humidified chamber at 37^{o}C for 1 hour with a solution of 10% FBS in PBS. After washing, slides were incubated for 1 hour with anti-Phospho-

Histone H2AX antibody (Upstate; 1:100) at 37^{o}C in humidified chamber. Secondary antibody was anti mouse IgG FITC conjugate (SIGMA) at the dilution 1:100. After washing and drying the slides mounting medium for fluorescence with DAPI (Vector Laboratories, Inc.) was used for counter staining.

Imaging Microscopy Analysis

The slides were examined using Nikon fluorescent microscope with DAPI/FITC/TRITC triple pass filters, images were captured using a CCD (charge-coupled device) camera and software (Smart capture VP), and data analysed.

siRNA

siRNA oligonucleotides were purchased from Dharmacon RNA Technologies. siRNA oligonucleotides used for WRN were 5' AAGGCAUGUGUUCGGAAGAUU3' and 3'UUUUCCGUACACAAGCCUUCU5'. For DNA ligase IIIα a target plus SMART pool were used. These oligonucleotides were transiently transfected into K562 cell lines using Cell Line Nucleofector Kit V (VCA-1003) in Nucleofector II Amaxa biosystems.

For transfection 10 μl of 20 μM siRNA were used for 1x10^{6} cells. At the time optimal for silencing of these genes (72 hours after transfection), cells were harvested either to proceed western blotting or DSB *in vivo* plasmid misrepair assay. Mock transfection and siRNA non-target were used as controls.

***In vivo* Plasmid Misrepair Assay**

*Eco*R1 (Fermentas) linearized pUC18 (Cat no. SD0051 from Fermentas) were transfected in siRNA non-target, siRNA silenced K562 and Artemis over-expressed K562 cells, using Amaxa Nucleofector Kit V. Plamid DNA was extracted and used to transform E. *coli* strain DH5α (Cat no. 18258-012 from Invitrogen) and the transformation mixture were plated onto agar plates containing X-gal and IPTG. Colonies were analyzed by counting the total number of white (misrepaired colonies) and Blue (properly repaired colonies). Misrepair frequency were calculated by the number of white colonies as a percentage

of total blue and white colonies. White colonies were characterized by PCR amplification using primers 5'CGGCATCAGAGCAGATTGTA3' and 5'TGGATAACCGTATTACCGCC3' (SIGMA Genosys) running 35 cycles at 60^{o}C and detected on 1% agarose gel. The same primers were used for sequencing of repaired plasmids.

Results

Reduced steady state levels of Artemis and DNA ligase IV in BCR-ABL positive CML cell lines.

BCR-ABL positive CML cells produce increased ROS [4] (**supplementary Figure 1**) that results in an increase in DSBs [3,5,6]. Notably, the repair of DSB is clearly abnormal in BCR-ABL positive CML cells, although the mechanism by which this altered repair occurs is unknown [3,5,6].

To examine the steady state levels of the key NHEJ proteins, including Ku70/86, DNA-PKcs, DNA ligase IV/XRCC4 and Artemis, western blotting analysis was performed in BCR-ABL positive CML cells and compared with controls. We find that the CML cell lines (K562, MEG01, KU812 and Kasumi 4) have significantly reduced steady state levels (4-7fold) of Artemis **(Figure 1Ai**), compared with three EBV-transformed B cell lines (NC3, NC10 and NC108), established from 3 different normal individuals, and a BCR-ABL negative leukemia cell line MO7e (**Figure 1Aii**). In addition, DNA ligase IV levels were 2-3-fold lower in CML cell lines, compared with appropriate controls (**Figure 1B**). Treatment of CML cells with the proteosome inhibitor MG132 had no effect on the levels of Artemis and DNA ligase IV, indicating that the reduced levels of these proteins in CML cells is not due to proteosomal degradation (data not shown).

Up-regulation of DNA ligase IIIα and WRN in BCR-ABL positive CML cell lines.

Recent studies have identified an "alternative or back-up" NHEJ repair, involving DNA repair proteins, such as, DNA ligase IIIα and PARP1, that is characterized by increased repair errors [25,32,35]. To

determine whether this "back-up" NHEJ may contribute to altered DSB repair in CML[36], we initially examined the steady state levels of candidate "back-up" repair proteins, such as, DNA ligase IIIα, XRCC1, and PARP1, in BCR-ABL positive CML cell lines (K562, MEG01, KU812 and Kasumi 4). The steady state levels of DNA ligase IIIα were significantly elevated (3-6-fold) in BCR-ABL positive cell lines, compared with control EBV-transformed B cell lines (NC3, NC10 and NC108) **(Figure 1C).** DNA ligase IIIα is also elevated in BCR-ABL positive CML, compared with BCR-ABL negative leukemia cell lines, U937 and MO7e (**Figure 1D**). Furthermore, the steady state level of DNA ligase IIIα is increased in MO7e cells stably expressing BCR-ABL (P210MO7e), compared with isogenic MO7e cells (**Figure 1D**). In contrast, there were no significant changes in the levels of the single strand break repair proteins, PARP1 and XRCC1, the partner protein of DNA ligase IIIα **(Figure 1C)**.

Next, we examined expression levels of WRN protein, a RecQ helicase with 3'-5' exonuclease activity that has been implicated in NHEJ repair [37-40]. Intriguingly, the steady state levels of WRN protein were also elevated (4-7-fold) in CML cell lines (K562, MEG01, KU812, Kasumi4) and P210MO7e, compared with control lymphoblastoid cell lines (NC3, NC10 and NC108) and the BCR-ABL negative leukemia cell lines, U937 and MO7e (**Figure 1C and D**).

To provide additional evidence for the relationship between DNA ligase IIIα and WRN and expression of the BCR-ABL, we examined the levels of these proteins in primary samples (N=4) from patients with different levels of BCR-ABL, following treatment with the tyrosine kinase inhibitor Gleevec (**supplementary Table 1**). Nuclear extracts from patient cells demonstrate that the steady state levels of WRN and DNA ligase IIIα are reduced in patient sample (CML1) where BCR-ABL levels (60%) are significantly decreased, as assessed by fluorescence in situ hybridization (FISH) (**Figure 1E, supplementary Table 1**). In contrast, the level of the Ku86 subunit does not change significantly (**Figure 1E**). These data, together with that in Figure 1D suggest that the increased steady state levels of

DNA ligase IIIα and WRN may either be a direct effect of BCR-ABL or a consequence of the increased levels of ROS and DNA damage caused by BCR-ABL expression.

WRN and DNA ligase IIIα co-localize with DRneo at ISce-1 induced DSBs

To investigate the role of WRN and DNA ligase IIIα in DSB repair in BCR-ABL positive CML, K562 and control NC10 cells were stably transfected with the DRneo plasmid that contains the ISce-1 restriction site that is not present in the mammalian genome (K562DRneo and NC10DRneo, **Figure 2A**)[41]. Subsequent transfection of these cells with expression constructs for ISce-1 endonuclease specifically induces a DSB into the genome of these cells [41]. A combined fluorescence *in situ* hybridization (FISH)-immunostaining technique was used to determine whether DNA ligase IIIα and WRN localize to the ISce-1 induced DSBs [34,42]. The efficiency of DSB induction, following transfection of the ISce-1 endonuclease, was determined by the nuclear co-localization of γH2AX, a key marker for DSBs, and the DRneo signal. Two hundred nuclei were analyzed from each of at least 3 experiments. Approximately 12% percent of K562DRneo (**Figure 2B, supplementary Figure 2B**) and 8% NC10DRneo (**supplementary Figure 2 A,B**) cells had induced DSB, as shown by co-localization of γ-H2AX and DRneo. In CML (**Figure 2B, supplementary Figure 2B**) 8% of cells show co-localization of Ku86 with DRneo vs 6% in NC10 cells, following I-Sce1 expression. In contrast, the co-localization of DNA ligase IV with DRneo (**Figure 2B, supplementary Figure 2B**) was significantly lower in CML cells (1%), compared with NC10 cells (4%). More strikingly, while we had difficulty detecting co-localization of either DNA ligase IIIα or WRN with DRneo in NC10 cells (**supplementary Figure 2 A,B**), DNA ligase IIIα and WRN (**Figure 2B, supplementary Figure 2B**) did co-localize with DRneo in K562 cells at a frequency of about 2%. Because the antibodies have different affinities for their target protein, it is not possible to compare the co-localization frequencies obtained with different antibodies. Nonetheless, this approach does reveal quantitative differences in the co-localization of a specific

protein in different cell lines and, importantly, showed that DNA ligase IIIα and WRN are specifically recruited to DSBs in CML cells, providing evidence that these proteins are participants in the altered DSB repair in these cells.

DNA ligase IIIα immunoprecipitates with WRN

To determine whether DNA ligase IIIα and WRN proteins associate in a complex, we performed immunoprecipitation experiments with WRN antibody. Notably, significantly higher amounts of DNA ligase IIIα were specifically co-immunoprecipitated from CML extracts compared with extracts from comparable control cell lines (**Figure 3A**). Similar results were obtained in reciprocal experiments using the DNA ligase IIIα antibody (**Figure 3B**). These data provide evidence for a novel complex containing WRN and DNA ligase IIIα that is present at higher levels in CML cells, compared with control cell lines.

siRNA down-regulation of WRN and DNA ligase IIIα results in increased DSBs.

In order to demonstrate that WRN and DNA ligase IIIα play a role in repairing DSBs in BCR-ABL positive CML, we examined whether their down-regulation results in an increased level of unrepaired DSB. Following siRNA knockdown of either WRN (approximately 90% reduction at 72 hours) or DNA ligase IIIα (approximately 75% reduction at 72 hours) in CML cells (**Figure 4A**), there was a significant increase ($p<0.01$) in the number of γH2AX foci (**Figure 4B, C, supplementary Table 2**). Together, these results suggest that both WRN and DNA ligase IIIα play a role in repair of endogenously generated DSBs in CML cells.

Next, we examined the role of WRN and DNA ligase IIIα in the repair of DSBs generated by exogenous agents in CML cells. The number of γH2AX foci was determined in K562 cells 6 hours after exposure to 2.5 Gy of γ-radiation. There was a marked defect in the repair of DSBs induced by ionizing radiation in cells with reduced levels of DNA ligase IIIα (**$p<0.01$**; **Figure 4B, C, supplementary Table 2**). In contrast, knockdown of WRN did not result in a significant increase in the number of γH2AX foci

(**Figure 4B, C, supplementary Table 2**), compared with non-target controls, but the foci were much larger and were similar to those remaining in DNA ligase IIIα knockdown cells.

Knockdown of DNA ligase IIIα and WRN decreases the end-joining efficiency in CML cells.

To more directly define the role of WRN and DNA ligase IIIα in the repair of DSB in CML, an *in vivo* plasmid end-joining assay was performed. Following knockdown of either WRN or DNA ligase IIIα, a pUC18 plasmid containing a DSB within LacZα was transfected into K562 cells. Circularized (repaired) plasmid DNA was extracted from K562 cells and used to transform E. coli, as previously reported [10]. Reducing the levels of either DNA ligase IIIα (**Figure 5A, supplementary Table 3**) or WRN (**Figure 6A, supplementary Table 3**) results in a 2-3 fold reduction in the number of colonies, indicating a decrease in end-joining efficiency in the BCR-ABL positive CML cells ($p<0.01$). Analysis of the colonies from the plasmid reactivation assays for their frequency of repair errors, i.e., white (incorrectly repaired) vs total colonies (blue [correctly repair]+ white)[10] , revealed that knockdown of DNA ligase IIIα results in a significant increase ($p<0.01$) in the frequency of misrepaired colonies (**Figure 5B, supplementary Table 3**). There was no significant change in the percentage of misrepair events that resulted in large deletions, defined as >20 bp (**Figure 5C, D, supplementary Table 3**). In contrast, knockdown of WRN did not increase the frequency of misrepaired colonies (**Figure 6B, supplementary Table 3**), but there was a significant ($p<0.01$) increase (approximately 3 fold) in the percentage of colonies with large deletions (**Figure 6C, D, supplementary Table 3**).

To determine whether knockdown of either DNA ligase IIIα or WRN leads to differences in repair utilizing DNA sequence microhomologies, we sequenced the breakpoint junctions of 15 repaired plasmids from each of the LacZα reactivation experiments. The majority (80%) of plasmids in K562 cells are repaired utilizing DNA microhomologies of 2 to 6 bp . In contrast, plasmids from cells with reduced levels of either DNA ligase IIIα (25%; $p<0.001$; **Figure 5E**) or WRN (40%; $p<0.001$; **Figure 6E**) had very short

or no sequence microhomologies at the breakpoint junctions in repaired plasmids (**Table 1**). Finally, we determined that siRNA knockdown of either WRN or DNA ligase IIIα in CML cells results in a small but reproducible decrease in viability as measured by trypan blue exclusion (**supplementary Figure 3**).

Artemis over-expression leads to a decreased in large deletions

To determine whether the reduced levels of Artemis contribute to the aberrant DSB repair in CML, Artemis was over-expressed in K562 cells (**Figure 7A**). Although Artemis over-expression did not significantly alter the end-joining efficiency (**Figure 7B**), it results in a considerable decrease in the size of DNA deletions at misrepaired DSB **(**$p<0.001$**; Figure 7C,D).** In addition, analysis of the breakpoint junctions from 15 repaired plasmids in K562 cells overexpressing Artemis show a decrease in repair using DNA sequence microhomologies down to 33%, compared with empty vector controls (80%) ($p<0.001$**; Figure 7E, Table 1**). Thus, down-regulation of Artemis in CML results in abnormal processing of DSBs.

Discussion

BCR-ABL has been shown to induce a cycle of events whereby increased ROS production leads to DSBs that are repaired by an error-prone mechanism. Here we have identified a novel protein complex containing DNA ligase IIIα and WRN that is involved in repair of DSBs in CML cells. This complex participates in an alternative end-joining pathway that compensates for the decreased activity of the major NHEJ pathway resulting from reduced levels of Artemis and DNA ligase IV, in CML. We suggest that alternative end-joining mediated by DNA ligase IIIα and WRN contributes to disease progression by enabling cells to repair ROS-induced DSBs albeit by a more error-prone pathway, ensuring the survival of CML cells at the cost of increased genomic instability.

Ku binding to DSBs is essential to initiate repair via the main NHEJ pathway [11]. Recent studies show that DNA-PKcs and DNA ligase IV are recruited independently to Ku-bound DSBs [43]. In addition to catalyzing the last step of the major NHEJ repair pathway [14], studies in yeast show that the DNA ligase IV homologue, Dnl4, acts early in NHEJ, stabilizing Ku binding and that, in the absence of Dnl4, there is increased end resection [44]. In BCR-ABL positive CML cells, we have shown that the steady state levels of DNA ligase IV are signficantly reduced. This suggests that Ku binding may be destabilized in CML cells, resulting in increased end resection. In addition, since DNA ligase IV performs the final ligation of DNA ends, the reduced levels of DNA ligase IV are likely to cause a delay in the joining of DNA ends synapsed by DNA PK. Such a delay may lead to the loss of a few additional nucleotides from the ends.

Here, we show that the steady state levels of DNA ligase IIIα are elevated in CML cells and is recruited to DSBs. This work provides further evidence that DNA ligase IIIα, which normally plays a role in the repair of DNA single strand breaks and BER [29,45], participates in a "back-up" pathway for NHEJ when DNA ligase IV levels are reduced [25,35]. Notably, knockdown of DNA ligase IIIα in CML cells results in an increased frequency of misrepair but has no effect on the size of deletions. Based on these results we propose that DNA ligase IIIα compensates for the reduced levels of DNA ligase IV by acting at DNA ends synapsed by DNA-PK. In addition, our data suggest that another ligase, possibly DNA ligase I completes the repair events generating the deletions.

In addition to DNA ligase IV, the level of another key factor in the major NHEJ pathway, Artemis is also markedly reduced in CML cells. Although the Artemis nuclease interacts with and is activated by DNA PKcs, it is thought to be only required for processing a subset of DSBs produced by such agents as ionizing radiation and ROS, defined as "complex" DSBs [17]. The reduced levels of Artemis do not appear to be caused by

proteosomal degradation and cannot be explained by changes in the level of DNA PKcs because, we find that, in contrast to the report of Deutsch et al [46], DNA PKcs is not reduced in CML cells. Notably, over-expression of Artemis in CML cell lines results in a reduction in the size of deletions. These results suggest that Artemis, in addition to participating in end processing, may play a role in stabilizing complexes containing DNA-PK that are assembled on DNA ends.

We find that the steady state levels of another DNA repair protein, WRN, are also elevated in BCR-ABL positive CML cells. Although WRN is not considered to be one of the core NHEJ factors, it does bind to Ku, thereby increasing its exonuclease activity[20-23]. However, the biological relevance of the stimulation of WRN nuclease activity by Ku is not obvious because cells lacking WRN protein are not hyper-sensitive to ionizing radiation like other NHEJ deficient cell lines and exhibit an increased incidence of deletions [24]. In addition, WRN is a substrate of the c-Abl kinase and is constitutively phosphorylated by BCR-ABL in CML cells, resulting in inhibition of exonuclease and helicase activities [47]. Here, we have shown that knockdown of WRN in CML cells leads to an increase in the size of deletions. Thus, it appears that WRN acts to protect DNA ends from nucleolytic resection. Presumably, the elevated levels of WRN in the CML cells reflect an attempt to prevent deletions at the ROS-induced DSBs. The mechanism by which WRN suppresses deletions is not known. It is possible that WRN stabilizes complexes of NHEJ proteins at DNA ends. Alternatively, WRN may negatively regulate the activity of nuclease(s) that act at DSBs, thereby limiting resection.

One of the standard methods for discriminating between the end-joining pathways used to repair DNA ends is to examine the sequences at the joins; alternative NHEJ repair appears to use microhomology-mediated repair at DNA ends [25-28]. CML cells repair approximately 80 percent of DNA ends using microhomologies. Knockdown of DNA ligase IIIα and WRN, and overexpression of Artemis, proteins specifically altered in

CML, lead to a significant reduction in microhomology sequences at end-joined sites. Furthermore, the size of microhomology sequences appear to decrease with these experimental maneuvers. These data provide additional evidence for an alternative end-joining pathway is operative in CML.

Abnormal repair of ROS-induced DSBs is a characteristic feature of BCR-ABL positive CML. Here, we have shown that both down-regulation of the major NHEJ pathway and up-regulation of an error-prone alternative NHEJ pathway contribute to the altered DNA repair and genomic instability in CML cells. The elevated levels of DNA ligase IIIα and WRN compensate for DNA ligase IV deficiency and suppress deletions, respectively. Since these proteins associate and co-localize to DSBs in CML cells, it seems likely that they functionally interact with DNA PK complexes formed at DNA ends. We suggest that the reduced levels of Artemis and/or DNA ligase IV results in decreased stability of DNA PK complexes at DNA ends that in turn results in increased end resection. The identity of the protein factors involved in the repair pathway acting on the resected ends and generating the deletions is not known. Nonetheless, it is evident that there are major differences in the repair of DSBs in BCR-ABL positive CML cells. Since resistance to Gleevec is being reported with greater frequency [53], this altered repair, in particular the alternative NHEJ pathway, constitutes an attractive target for the development of novel therapeutic strategies for CML. Thus, further characterization of the abnormal DNA repair in BCR-ABL positive CML will not only provide insights into the role of genomic instability in disease progression, but will also lay the groundwork for therapeutic strategies in patients resistant to tyrosine kinase inhibitors.

Acknowledgements

We would like to thank Professor Stephen Baylin (JHU) for insightful comments and careful reading of our manuscript. We thank Matt Whitehurst for technical support. We thank Drs Rapoport (UMaryland)

and Douglas Smith (JHU) for CML patient samples (IRB H25314). FR and AS are funded by the Cigarette restitution Funds of Maryland and the Leukemia Lymphoma Society. AT is funded by NIH grants (ES 012512).

Authorship

AS designed and performed the experiments, analyzed the data and participated in writing the paper. FR designed the experiments, analyzed the data and wrote the paper. AT provided reagents and critical reading of the manuscript.

Figure Legends

1 BCR-ABL positive CML cell lines show down-regulation of major NHEJ proteins, Artemis and DNA ligase IV, and upregulation of alternative NHEJ proteins, DNA ligase IIIα and WRN.

A(i) Western blotting using nuclear extracts from two BCR-ABL positive CML cell lines (K562 and MEG01), and three EBV transformed B cell lines, established from normal individuals (NC3, NC10 and NC108), and (**ii**) one BCR-ABL negative CML cell line (MO7e). Artemis shows down-regulation (4-7 fold) in BCR-ABL positive CML cell lines. Either Actin or Ku86 were used as loading controls. **B**: Western blotting using nuclear extracts from K562 shows 2-3 fold decrease in DNA ligase IV expression, compared with EBV transformed B cell lines (NC3 and NC10). Ku86 was used as loading control. **C:** Western blotting using nuclear extracts from two BCR-ABL positive CML cell lines (K562 and MEG01) and three EBV transformed B cell lines (NC3, NC10 and NC108). CML cell lines show up-regulation of DNA ligase IIIα (3-6 fold). PARP1 expression is unchanged. Werner's Syndrome protein, WRN shows up-regulation (4-7 fold) in CML cell lines. Actin was used as loading control. **D**: BCR-ABL negative MO7e shows down-regulation of DNA ligase IIIα and WRN compared with BCR-ABL positive P210MO7e and K562. Western blotting using nuclear extracts from two BCR-ABL positive cell lines (K562 and P210MO7e) and BCR-ABL negative cell lines (U937 and MO7e). Actin was used as loading control. **E**: Primary CML bone marrow mononuclear cells show down-regulation of DNA ligase IIIα and WRN. Western blotting using nuclear extracts from CML cell line (K562) and two CML patients (CML1 and 2) post Gleevec treatment (6-12 months). Patient CML1 shows decreased DNA ligase IIIα and WRN expression with decreased levels of BCR-ABL positivity by FISH. Patient CML2 shows increase expression of DNA ligase IIIα and WRN, with 100% BCR-ABL positivity. BCR-ABL positive CML cell line K562 was used as a positive control. Ku86 and Actin were used as loading controls.

2 PCR and FISH localization of the DRneo probe in K562DRneo and NC10DRneo cells.

A(**i**): Detection of integrated DRneo in K562 and NC10 cell clones stably transfected with DRneo (K562DRneo and NC10DRneo, respectively) by PCR. (**ii**): The DRneo construct labeled with spectrum red was used for FISH analysis of metaphase spreads prepared from K562DRneo cells. The DRneo was integrated at a telomeric position on the chromosomes as shown in DAPI stained (left, red arrow) and G-banded (middle, red arrow) images. Two-color FISH was used to localize DRneo to chromosome 4 in K562DRneo cells (right image). Chromosomes from two different metaphase cells shown with yellow signal indicating chromosome 4 alpha satellite probe, localized to the centromere (black arrow) and red signal localizing the DRneo probe to the telomeric region of the chromosome (red arrow). **B**: Co-localization of DRneo and γH2AX, Ku86, DNA ligase IV, DNA ligase IIIα, and WRN in K562DRneo cells by FISH. Images show co-localization of DRneo (FITC, green signal) and above mentioned proteins (TRITC, red signal) in K562DRneo cells transfected with ISce-1. Nuclei are stained with DAPI (blue). Right hand panels are merged images of FITC and TRITC showing co-localization.

3 DNA ligase IIIα immunoprecipitates with WRN.

Nuclear extracts from CML cell line K562 and EBV transformed B cell line NC10 were used to immunoprecipitate, **(A)** DNA ligase IIIα, using WRN antibody, followed by Western blotting for DNA ligase IIIα (upper panel) and WRN (lower panel) **(B)** Reciprocal immunoprecipitation of WRN, using DNA ligase IIIα antibody, followed by Western blotting for WRN (upper panel) and DNA ligase IIIα (lower panel). Western blotting was also performed for negative control non-specific antibodies.

4 siRNA down-regulation of WRN and DNA ligase IIIα in CML cell line.

A: Nuclear extracts were prepared at 4 different time points 0h, 24h, 48h and 72h. Western blotting was performed using WRN antibody (90% knockdown; upper panel) and DNA ligase IIIα antibody (75%

knockdown; middle panel). siRNA using non-target oligonucleotides were used as controls. Ku86 was used as loading control (lower panel). **B.** Bar graph showing the percentage of K562 cells with more than 5 γH2AX foci examined in siRNA non-target, siRNA knockdown of WRN and DNA ligase IIIα cells with or without irradiation (IR; 2.5 Gy). Black bars indicate no IR and grey bars are with IR treatment. 200 nuclei were examined from each of 3 different experiments. Values significantly different are marked with an asterisk ($p<0.01$ by Student's t-test). Error bars reflect the standard error of the mean. **C.** Images of three different cells showing γH2AX foci (FITC, green signal) in K562 following siRNA non-target (left panels), siRNA down-regulation of WRN (middle panels) and DNA ligase IIIα (right panels), with and without irradiation.

5 Down-regulation of DNA ligase IIIα decreases the end-joining efficiency and repair using DNA sequence microhomologies, but increases the misrepair frequency and has no effect on the percentage of large deletions.

An *in vivo* LacZα plasmid reactivation assay was used to measure end-joining in siRNA DNA ligase IIIα down-regulated cells and compared with that using siRNA controls. **A**: Relative percentage of colonies, indicating the efficiency of end-joining. **B**: The percentage of misrepair, i.e. the number of white colonies as a percentage of total colonies (blue+white). **C.** Graph of percentage large deletions, defined as > 20bp. **D.** Agarose gel showing PCR products of repaired colonies in siRNA non-target controls and siRNA knockdown of DNA ligase IIIα. **E:** The percentage of plasmids repaired using DNA sequence microhomologies of 2-6bp. Fifteen plasmids were sequenced Values significantly different are marked with an asterisk by Student's t-test ($p<0.01$ for A and B and $p<0.001$ for E). Error bars reflect the standard error of the mean.

.

6 Down-regulation of WRN decreases the efficiency of end-joining and repair using DNA sequence microhomologies but increases large deletions in misrepaired plasmids.

An *in vivo* LacZα plasmid reactivation assay was used to measure end-joining in siRNA down-regulated WRN K562 cells compared with that using siRNA controls. **A**: Relative percentage of colonies indicating the efficiency of end-joining. **B**: The percentage of misrepair, i.e. the percentage of the white colonies as a percentage of total colonies (blue+white). **C.** The percentage of large deletions, defined as > 20bp. **D.** Agarose gel showing PCR products of repaired colonies. **E:** The percentage of plasmids repaired using DNA sequence microhomologies of 2-6bp. Fifteen plasmids were sequenced. Values significantly different are marked with an asterisk by Student's t-test ($p<0.01$ for A and $p<0.001$ for C and E). Error bars reflect the standard error of the mean.

7: **Artemis over-expression in K562 leads to a decreased large deletions.**

A: Western blotting in K562 cells transfected with the myc-tagged Artemis cDNA construct (pcDNA huASC1D) showing Artemis over-expression. Ku86 was used as loading control. An *in vivo* LacZα plasmid reactivation assay was used to measure end-joining in Artemis over-expressed cells, compared with empty vector transfected controls. **B**: Relative percentage of colonies, indicating the efficiency of end-joining. **C.** Graph of percentage large deletions, defined as > 20bp. **D.** Agarose gel showing PCR products of repaired colonies in empty vector controls and Artemis overexpressed K562 cells. **E:** The percentage of plasmids repaired using DNA sequence microhomologies of 2-6bp. Fifteen plasmids were sequenced. Values significantly different are marked with an asterisk by Student's t-test ($p<0.001$ for C and E). Error bars reflect the standard error of the mean.

References

1. Druker BJ, Sawyers CL, Capdeville R, Ford JM, Baccarani M, Goldman JM. Chronic myelogenous leukemia. Hematology (Am Soc Hematol Educ Program). 2001:87-112.
2. Sawyers CL. Signal transduction pathways involved in BCR-ABL transformation. Baillieres Clin Haematol. 1997;10:223-231.
3. Rassool FV. Genetic rearrangements beget genomic instability. Blood. 2004;104:3424-3425.
4. Sattler M, Verma S, Shrikhande G, et al. The BCR/ABL tyrosine kinase induces production of reactive oxygen species in hematopoietic cells. J Biol Chem. 2000;275:24273-24278.
5. Skorski T. BCR/ABL regulates response to DNA damage: the role in resistance to genotoxic treatment and in genomic instability. Oncogene. 2002;21:8591-8604.
6. Nowicki M, R. F, Koptyra M, et al. BCR/ABL oncogenic kinase promotes unfaithful repair of the reactive oxygen species-dependent DNA double strand breaks. Blood. 2004;104:3746-3753.
7. Majsterek I, Blasiak J, Mlynarski W, Hoser G, Skorski T. Does the bcr/abl-mediated increase in the efficacy of DNA repair play a role in the drug resistance of cancer cells? Cell Biol Int. 2002;26:363-370.
8. Slupianek A, Hoser G, Majsterek I, et al. Fusion tyrosine kinases induce drug resistance by stimulation of homology-dependent recombination repair, prolongation of G(2)/M phase, and protection from apoptosis. Mol Cell Biol. 2002;22:4189-4201.
9. Brady N, Gaymes TJ, Cheung M, Mufti GJ, Rassool FV. Increased error-prone NHEJ activity in myeloid leukemias is associated with DNA damage at sites that recruit key nonhomologous end-joining proteins. Cancer Res. 2003;63:1798-1805.

10. Gaymes TJ, Mufti GJ, Rassool FV. Myeloid leukemias have increased activity of the nonhomologous end-joining pathway and concomitant DNA misrepair that is dependent on the Ku70/86 heterodimer. Cancer Res. 2002;62:2791-2797.
11. Falzon M, Fewell JW, Kuff EL. EBP-80, a transcription factor closely resembling the human autoantigen Ku, recognizes single- to double-strand transitions in DNA. J Biol Chem. 1993;268:10546-10552.
12. Gottlieb TM, Jackson SP. The DNA-dependent protein kinase: requirement for DNA ends and association with Ku antigen. Cell. 1993;72:131-142.
13. Mimori T, Hardin JA. Mechanism of interaction between Ku protein and DNA. J Biol Chem. 1986;261:10375-10379.
14. Grawunder U, Wilm M, Wu X, et al. Activity of DNA ligase IV stimulated by complex formation with XRCC4 protein in mammalian cells. Nature. 1997;388:492-495.
15. Roth DB, Porter TN, Wilson JH. Mechanisms of nonhomologous recombination in mammalian cells. Mol Cell Biol. 1985;5:2599-2607.
16. Roth DB, Wilson JH. Nonhomologous recombination in mammalian cells: role for short sequence homologies in the joining reaction. Mol Cell Biol. 1986;6:4295-4304.
17. Jeggo PA, Lobrich M. Artemis links ATM to double strand break rejoining. Cell Cycle. 2005;4:359-362.
18. Hickson ID. RecQ helicases: caretakers of the genome. Nat Rev Cancer. 2003;3:169-178.
19. Bachrati CZ, Hickson ID. RecQ helicases: suppressors of tumorigenesis and premature ageing. Biochem J. 2003;Pt.

20. Orren DK, Machwe A, Karmakar P, Piotrowski J, Cooper MP, Bohr VA. A functional interaction of Ku with Werner exonuclease facilitates digestion of damaged DNA. Nucleic Acids Res. 2001;29:1926-1934.

21. Cooper MP, Machwe A, Orren DK, Brosh RM, Ramsden D, Bohr VA. Ku complex interacts with and stimulates the Werner protein. Genes Dev. 2000;14:907-912.

22. Li B, Comai L. Functional interaction between Ku and the werner syndrome protein in DNA end processing. J Biol Chem. 2000;275:28349-28352.

23. Li B, Comai L. Requirements for the nucleolytic processing of DNA ends by the Werner syndrome protein-Ku70/80 complex. J Biol Chem. 2001;276:9896-9902.

24. Oshima J, Huang S, Pae C, Campisi J, Schiestl RH. Lack of WRN results in extensive deletion at nonhomologous joining ends. Cancer Res. 2002;62:547-551.

25. Wang H, Rosidi B, Perrault R, et al. DNA ligase III as a candidate component of backup pathways of nonhomologous end joining. Cancer Res. 2005;65:4020-4030.

26. Corneo B, Wendland RL, Deriano L, et al. Rag mutations reveal robust alternative end joining. Nature. 2007;449:483-486.

27. Klassen R, Krampe S, Meinhardt F. Homologous recombination and the yKu70/80 complex exert opposite roles in resistance against the killer toxin from Pichia acaciae. DNA Repair (Amst). 2007;6:1864-1875.

28. Yan CT, Boboila C, Souza EK, et al. IgH class switching and translocations use a robust non-classical end-joining pathway. Nature. 2007;449:478-482.

29. Gottlich B, Reichenberger S, Feldmann E, Pfeiffer P. Rejoining of DNA double-strand breaks in vitro by single-strand annealing. Eur J Biochem. 1998;258:387-395.

30. Riballo E, Critchlow SE, Teo SH, et al. Identification of a defect in DNA ligase IV in a radiosensitive leukaemia patient. Curr Biol. 1999;9:699-702.

31. Difilippantonio MJ, Zhu J, Chen HT, et al. DNA repair protein Ku80 suppresses chromosomal aberrations and malignant transformation. Nature. 2000;404:510-514.

32. Wang M, Wu W, Wu W, et al. PARP-1 and Ku compete for repair of DNA double strand breaks by distinct NHEJ pathways. Nucleic Acids Res. 2006;34:6170-6182.

33. Liang F, Han M, Romanienko PJ, Jasin M. Homology-directed repair is a major double-strand break repair pathway in mammalian cells. Proc Natl Acad Sci U S A. 1998;95:5172-5177.

34. Rassool FV, Le Beau MM, Shen ML, et al. Direct cloning of DNA sequences from the common fragile site region at chromosome band 3p14.2. Genomics. 1996;35:109-117.

35. Wang H, Perrault AR, Takeda Y, Qin W, Iliakis G. Biochemical evidence for Ku-independent backup pathways of NHEJ. Nucleic Acids Res. 2003;31:5377-5388.

36. Gaymes TJ, North PS, Brady N, Hickson ID, Mufti GJ, Rassool FV. Increased error-prone non homologous DNA end-joining--a proposed mechanism of chromosomal instability in Bloom's syndrome. Oncogene. 2002;21:2525-2533.

37. Mohaghegh P, Karow JK, Brosh Jr RM, Jr., Bohr VA, Hickson ID. The Bloom's and Werner's syndrome proteins are DNA structure-specific helicases. Nucleic Acids Res. 2001;29:2843-2849.

38. Perry JJ, Yannone SM, Holden LG, et al. WRN exonuclease structure and molecular mechanism imply an editing role in DNA end processing. Nat Struct Mol Biol. 2006.

39. Li B, Comai L. Displacement of DNA-PKcs from DNA ends by the Werner syndrome protein. Nucleic Acids Res. 2002;30:3653-3661.

40. Karmakar P, Snowden CM, Ramsden DA, Bohr VA. Ku heterodimer binds to both ends of the Werner protein and functional interaction occurs at the Werner N-terminus. Nucleic Acids Res. 2002;30:3583-3591.

41. Richardson C, Jasin M. Coupled homologous and nonhomologous repair of a double-strand break preserves genomic integrity in mammalian cells. Mol Cell Biol. 2000;20:9068-9075.

42. Rassool FV, North PS, Mufti GJ, Hickson ID. Constitutive DNA damage is linked to DNA replication abnormalities in Bloom's syndrome cells. Oncogene. 2003;22:8749-8757.

43. Mari PO, Florea BI, Persengiev SP, et al. Dynamic assembly of end-joining complexes requires interaction between Ku70/80 and XRCC4. Proc Natl Acad Sci U S A. 2006;103:18597-18602.

44. Zhang Y, Hefferin ML, Chen L, et al. Role of Dnl4-Lif1 in nonhomologous end-joining repair complex assembly and suppression of homologous recombination. Nat Struct Mol Biol. 2007;14:639-646.

45. Tomkinson AE, Vijayakumar S, Pascal JM, Ellenberger T. DNA ligases: structure, reaction mechanism, and function. Chem Rev. 2006;106:687-699.

46. Deutsch E, Dugray A, AbdulKarim B, et al. BCR-ABL down-regulates the DNA repair protein DNA-PKcs. Blood. 2001;97:2084-2090.

47. Cheng WH, von Kobbe C, Opresko PL, et al. Werner syndrome protein phosphorylation by abl tyrosine kinase regulates its activity and distribution. Mol Cell Biol. 2003;23:6385-6395.

48. Boldogh I, Roy G, Lee MS, et al. Reduced DNA double strand breaks in chlorambucil resistant cells are related to high DNA-PKcs activity and low oxidative stress. Toxicology. 2003;193:137-152.

49. Slupphaug G, Kavli B, Krokan HE. The interacting pathways for prevention and repair of oxidative DNA damage. Mutat Res. 2003;531:231-251.

50. Riballo E, Doherty AJ, Dai Y, et al. Cellular and biochemical impact of a mutation in DNA ligase IV conferring clinical radiosensitivity. J Biol Chem. 2001;276:31124-31132.

51. Puebla-Osorio N, Lacey DB, Alt FW, Zhu C. Early embryonic lethality due to targeted inactivation of DNA ligase III. Mol Cell Biol. 2006;26:3935-3941.

52. Tebbs RS, Thompson LH, Cleaver JE. Rescue of Xrcc1 knockout mouse embryo lethality by transgene-complementation. DNA Repair (Amst). 2003;2:1405-1417.

53. Kantarjian H, O'Brien S, Talpaz M, et al. Outcome of patients with Philadelphia chromosome-positive chronic myelogenous leukemia post-imatinib mesylate failure. Cancer. 2007.

Fig 1

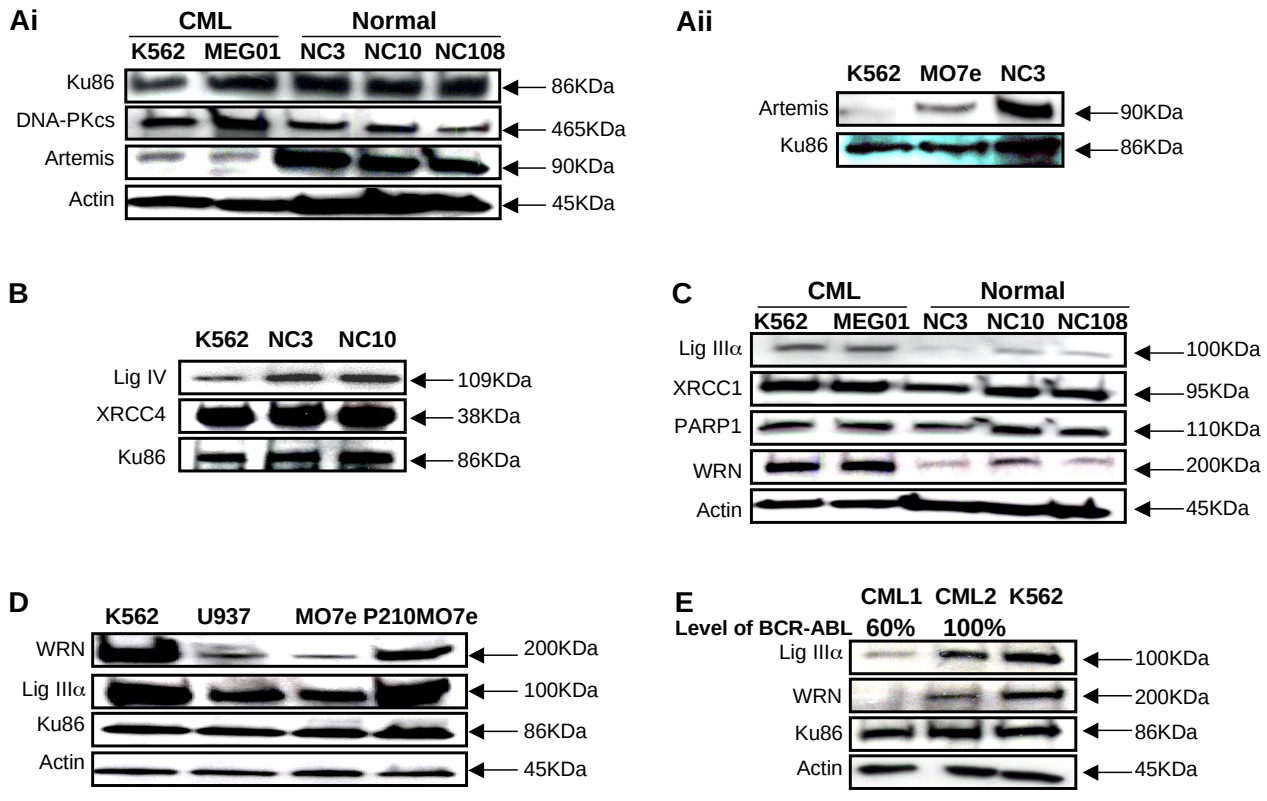
Ai
CML
Normal
K562 MEG01 NC3 NC10 NC108
Ku86
DNA-PKcs
Artemis
Actin
86KDa
465KDa
90KDa
45KDa
Aii
K562 MO7e NC3
Artemis
Ku86
90KDa
86KDa
B
K562 NC3 NC10
Lig IV
XRCC4
Ku86
109KDa
38KDa
86KDa
C
CML
Normal
K562 MEG01 NC3 NC10 NC108
Lig IIIα
XRCC1
PARP1
WRN
Actin
100KDa
95KDa
110KDa
200KDa
45KDa
D
K562 U937 MO7e P210MO7e
WRN
Lig IIIα
Ku86
Actin
200KDa
100KDa
86KDa
45KDa
E
CML1 CML2 K562
Level of BCR-ABL 60% 100%
Lig IIIα
WRN
Ku86
Actin
100KDa
200KDa
86KDa
45KDa

Fig 2

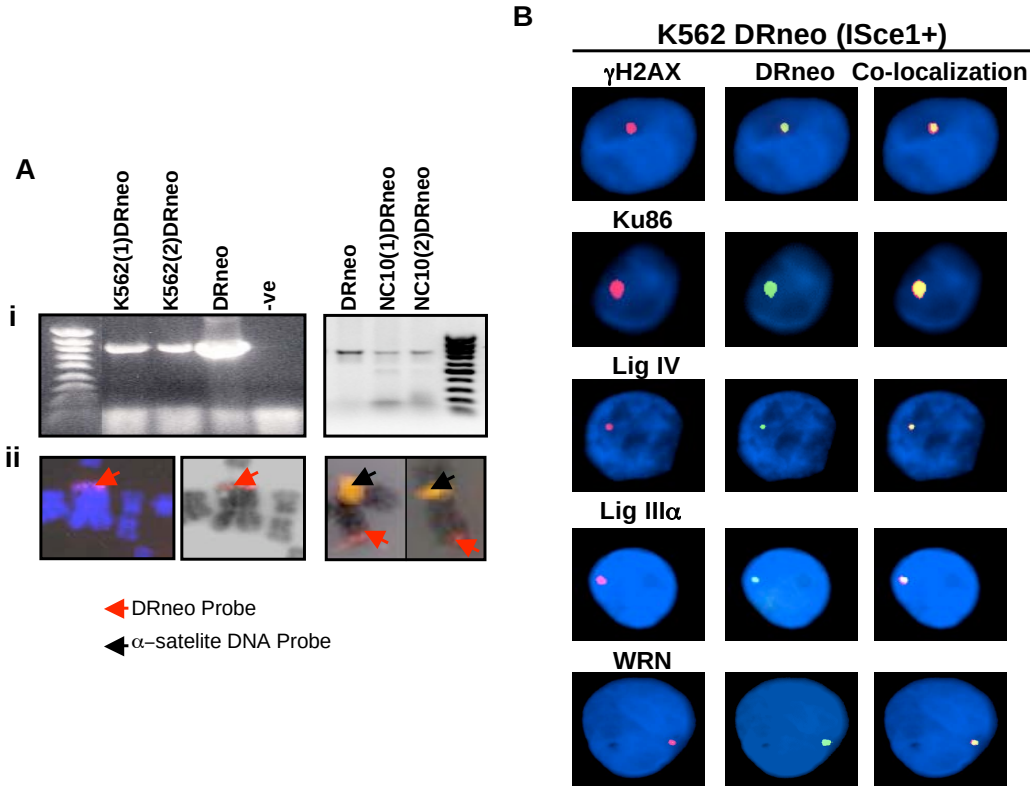
A
K562(1)DRneo
K562(2)DRneo
DRneo
-ve
DRneo
NC10(1)DRneo
NC10(2)DRneo
i
ii
DRneo Probe
α–satelite DNA Probe
B
K562 DRneo (ISce1+)
γH2AX
DRneo
Co-localization
Ku86
Lig IV
Lig IIIα
WRN

Fig 3

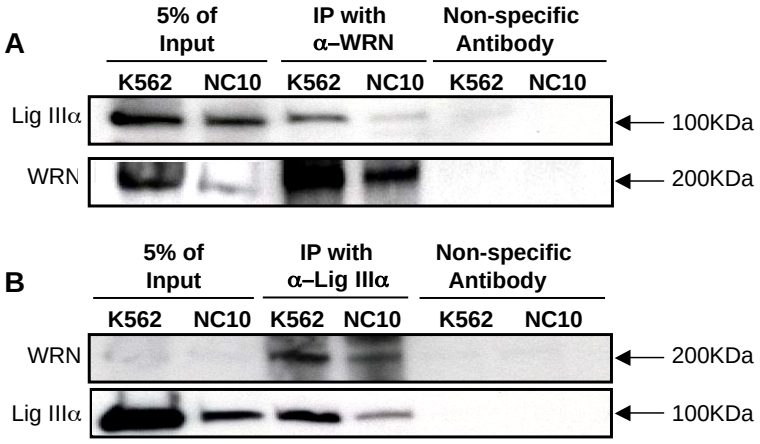
A
5% of Input
IP with α–WRN
Non-specific Antibody
K562
NC10
K562
NC10
K562
NC10
Lig IIIα
100KDa
WRN
200KDa
B
5% of Input
IP with α–Lig IIIα
Non-specific Antibody
K562
NC10
K562
NC10
K562
NC10
WRN
200KDa
Lig IIIα
100KDa

Fig 4

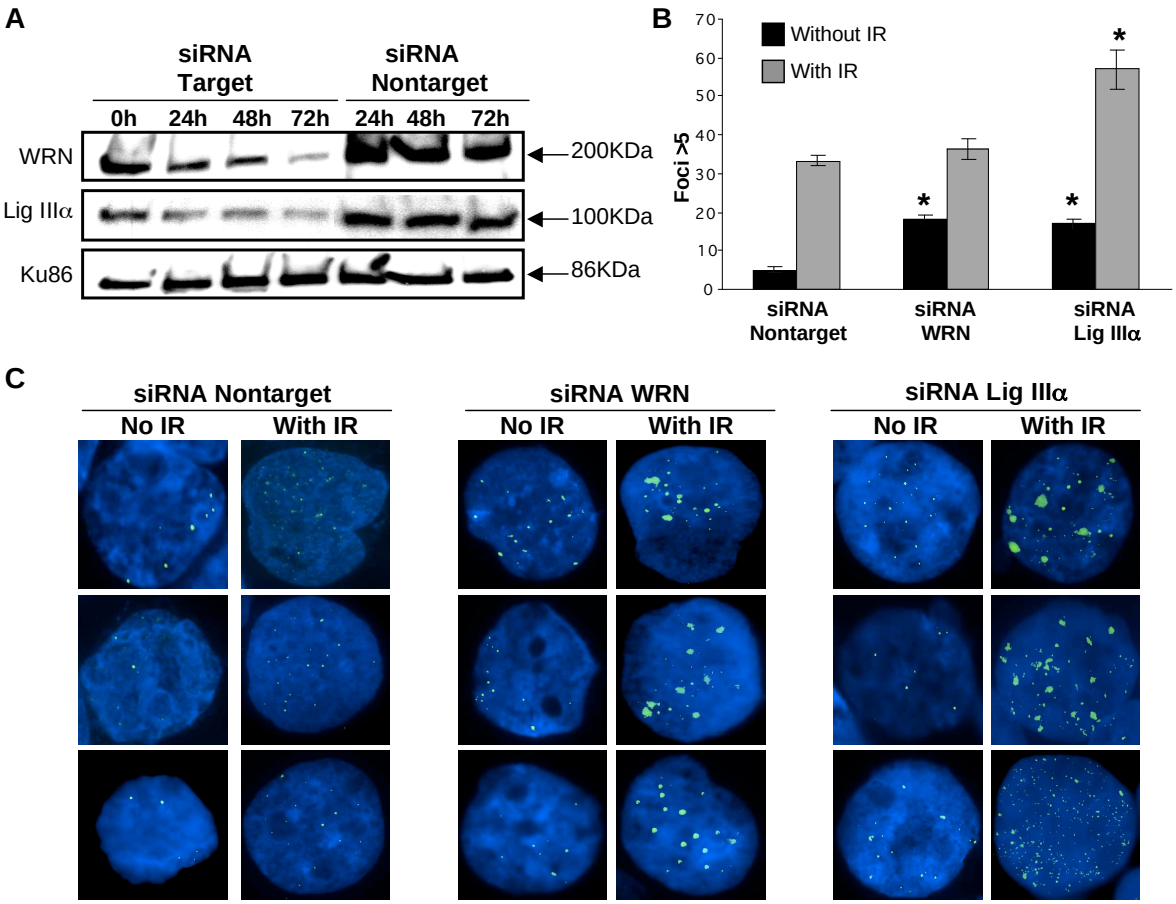
A
siRNA Target
siRNA Nontarget
0h 24h 48h 72h 24h 48h 72h
WRN
Lig IIIα
Ku86
200KDa
100KDa
86KDa
B
Without IR
With IR
Foci >5
0 10 20 30 40 50 60 70
*
*
*
siRNA Nontarget
siRNA WRN
siRNA Lig IIIα
C
siRNA Nontarget
siRNA WRN
siRNA Lig IIIα
No IR
With IR
No IR
With IR
No IR
With IR

Fig 5

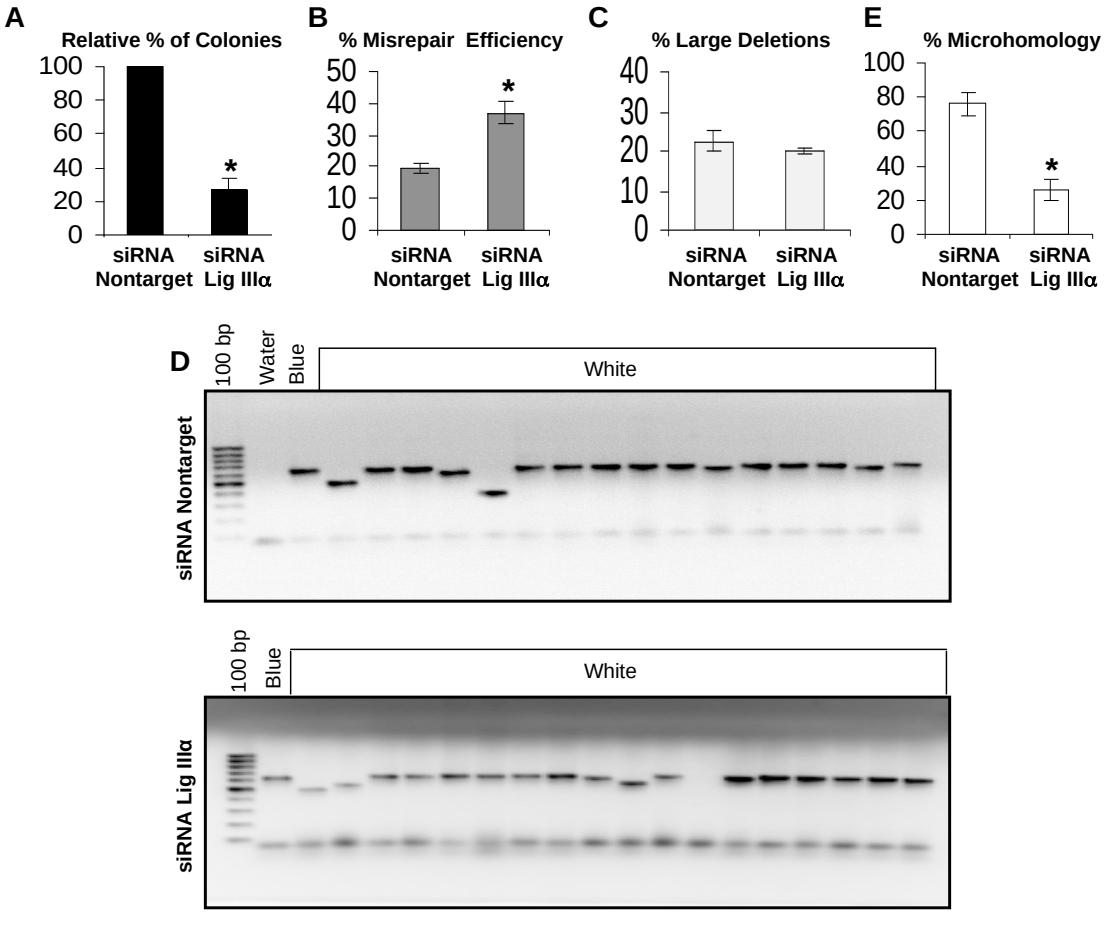
A
Relative % of Colonies
100
80
60
40
20
0
*
siRNA Nontarget
siRNA Lig IIIα
B
% Misrepair Efficiency
50
40
30
20
10
0
*
siRNA Nontarget
siRNA Lig IIIα
C
% Large Deletions
40
30
20
10
0
siRNA Nontarget
siRNA Lig IIIα
E
% Microhomology
100
80
60
40
20
0
*
siRNA Nontarget
siRNA Lig IIIα
D
100 bp
Water
Blue
White
siRNA Nontarget
100 bp
Blue
White
siRNA Lig IIIα

Fig 6

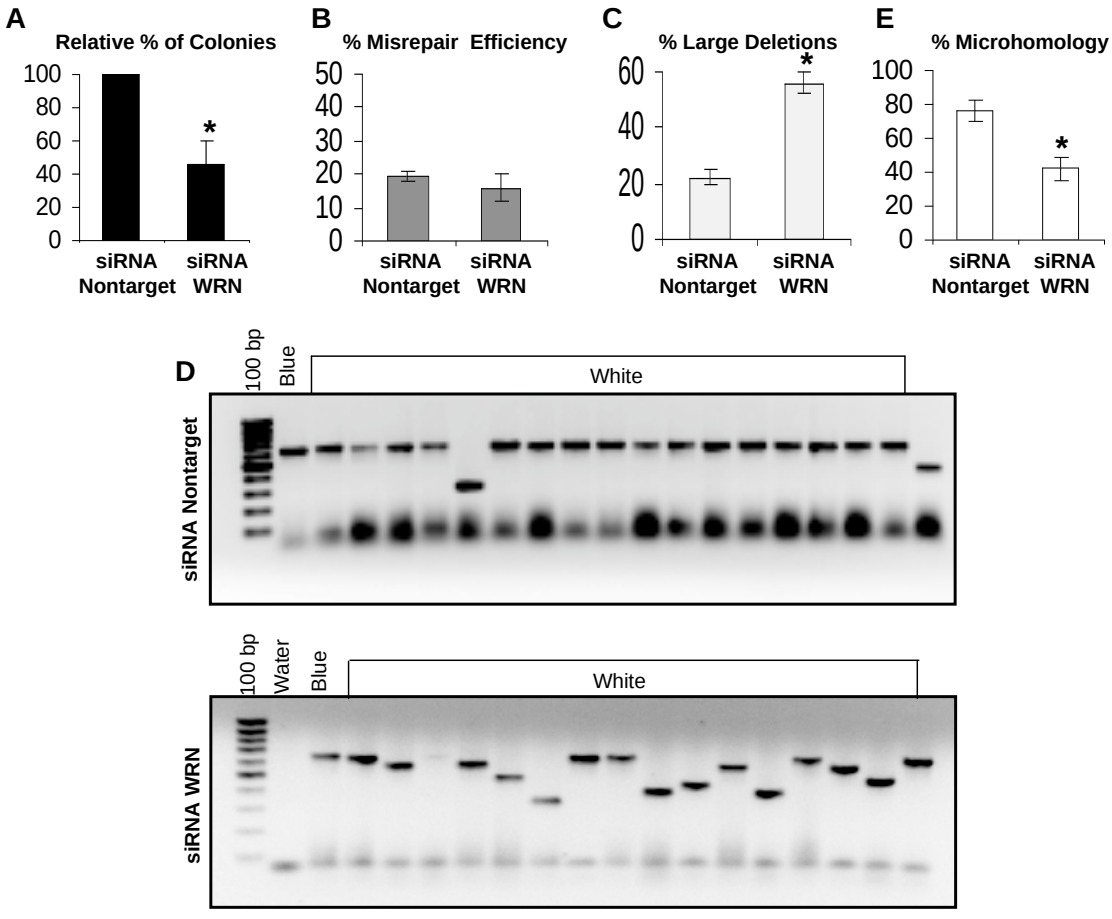
A
Relative % of Colonies
100
80
60
40
20
0
*
siRNA Nontarget
siRNA WRN
B
% Misrepair Efficiency
50
40
30
20
10
0
siRNA Nontarget
siRNA WRN
C
% Large Deletions
60
40
20
0
*
siRNA Nontarget
siRNA WRN
E
% Microhomology
100
80
60
40
20
0
*
siRNA Nontarget
siRNA WRN
D
100 bp
Blue
White
siRNA Nontarget
100 bp
Water
Blue
White
siRNA WRN

Fig 7

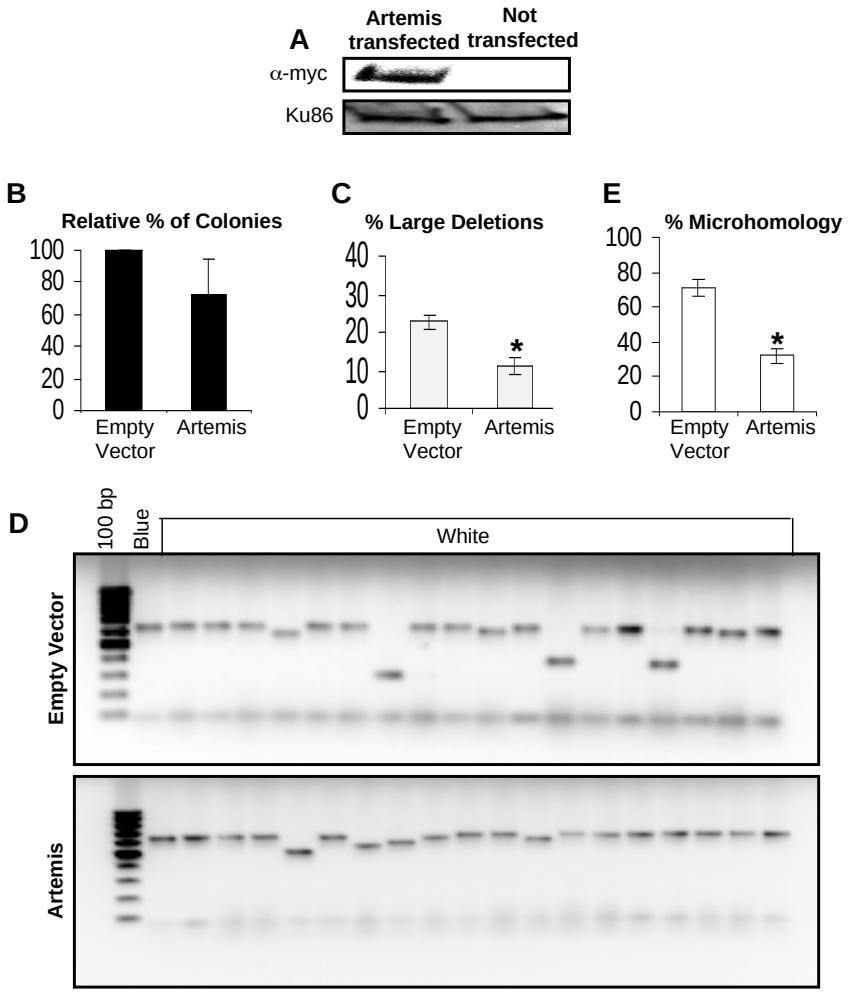
A
Artemis transfected
Not transfected
α-myc
Ku86
B
Relative % of Colonies
100
80
60
40
20
0
Empty Vector
Artemis
C
% Large Deletions
40
30
20
10
0
*
Empty Vector
Artemis
E
% Microhomology
100
80
60
40
20
0
*
Empty Vector
Artemis
D
100 bp
Blue
White
Empty Vector
Artemis

pUC18 first 780 bp

1 tcgcgcgttt cggtgatgac ggtgaaaacc tctgacacat gcagctcccg gagacggtca
61 cagcttgtct gtaagcggat gccgggagca gacaagcccg tcagggcgcg tcagcgggtg
121 ttggcgggtg tcggggctgg cttaactatg **cggcatcaga gcagattgta** ctgagagtgc
181 accatatgcg gtgtgaaata ccgcacagat gcgtaaggag aaaataccgc atcaggcgcc
241 attcgccatt caggctgcgc aactgttggg aagggcgatc ggtgcgggcc tcttcgctat
301 tacgccagct ggcgaaaggg ggatgtgctg caaggcgatt aagttgggta acgccagggt
361 tttcccagtc acgacgttgt aaaacgacgg ccagtgccaa gcttgcatgc ctgcaggtcg
421 actctagagg atccccgggt accgagctc***g aattcg***taat catggtcata gctgtttcct
481 gtgtgaaatt gttatccgct cacaattcca cacaacatac gagccggaag cataaagtgt
541 aaagcctggg gtgcctaatg agtgagctaa ctcacattaa ttgcgttgcg ctcactgccc
601 gctttccagt cgggaaacct gtcgtgccag ctgcattaat gaatcggcca acgcgcgggg
661 agaggcggtt tgcgtattgg gcgctcttcc gcttcctcgc tcactgactc gctgcgctcg
721 gtcgttcggc tgcggcgagc ggtatcagct cactcaaa**gg cggtaatacg gttatcca**ca

Forward Primer: **cggcatcaga gcagattgta** Reverse Primer: **gg cggtaatacg gttatcca**' EcoR1 Site: ***g aattcg***

Table 1: Representative sequenced clones from *in vivo* end-joining assay

*No of Clones	Sequence at the junction	No. of bp deleted	Microhomology
	siRNA Control		
K1	CGACGGCCAG/AGCCTGGGGT 394/543	148	GCC or AG
K2	GGATCC/GAAATTGTTATCCG 434/485	50	no microhomology
K3	GCGCAAGTGT/AAGTGTAAAG 266/535	268	AAGTGT
K4	ACCGAGCTCG/TTCCTGTGTG 450/476	25	no microhomology
K5	CCCGGGTACC/CCTGTGTGAA 443/478	34	CC
	siRNA WRN		
W1	GACTCTAGAG/GTTGCGCTCA 429/585	155	G
W2	CAGGCTGCGC/GAGTGAGCT 259/560	300	no microhomology
W3	AAAGGGGGAT/CTAACTCACA 324/567	242	no microhomology
W4	GGGGATGTGC/GAAGCATAA 328/527	198	no microhomology
W5	CCCGGGTACC/CCCGCTTTCC 443/598	154	CC
	siRNA DNA Ligase IIIa		
L1	GTAAAACGACGGC/TGTAAAG 391/538	146	no microhomology
L2	ATGCCTGCAG/CGAGCCGGAA 416/520	103	no microhomology
L3	ACCGAGCTCG/CGTCATAGCT 450/464	13	CG
L4	GCTCGAATTC/TTCCTGTGTG 455/476	20	TCC
L5	CGAGCTCGA/TTGTAATCAT 452	1	no microhomology
	Over-expression of Artemis		
A1	TACGCCAGCT/TCGTAATCAT 310/454	143	T
A2	GGCCAGTGCC/TATCCGCTCA 398/493	94	no microhomology
A3	GTCGACTCTA/TATCCGCTCA 426/493	66	TA
A4	GAGCTCGAAT/TCCTGTGTGA 453/477	23	T
A5	CGAGCTCGAA/TGGTCATAGC 453	10	no microhomology

* 15 colonies were sequenced from each individual experiments.

Supplementary Figure 1

<u>K562 shows higher level of ROS compared to NC10</u>

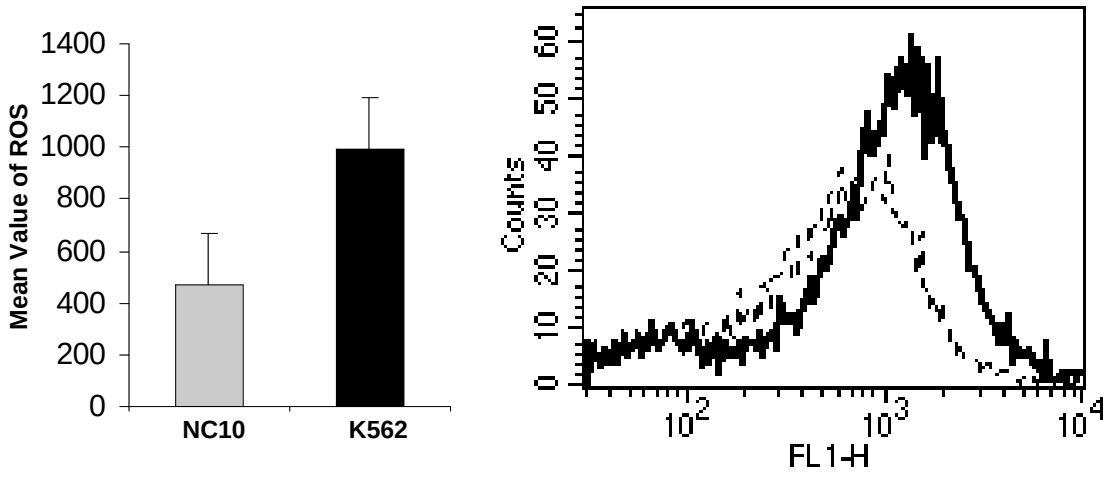

Intracellular ROS level were determined by using the probe 2,7-dichlorodihydro-fluorescein diacetate (H2DCF-DA, Invitrogen, Carlsbad, CA). Cells ($1x10^6$) were treated in the presence of the probe to a final concentration of 10 µM and incubated at 37°C for 10 minutes. ROS levels were determined by flow cytometry (Becton Dickinson FACScan).

Supplementary Figure 2

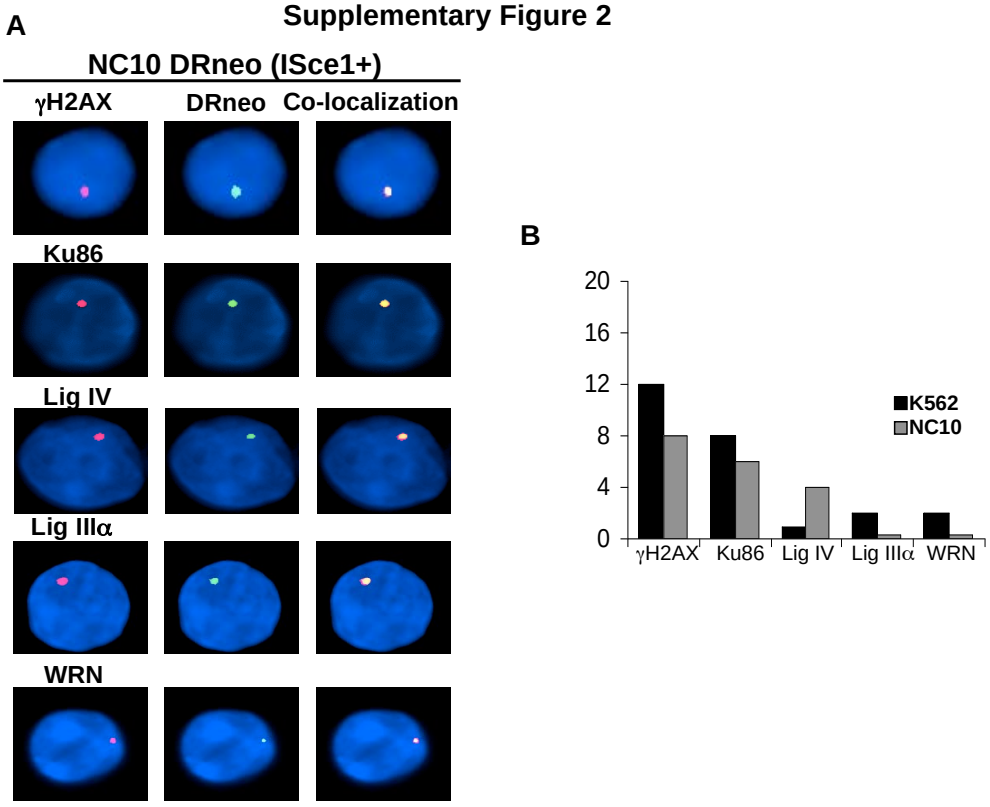

A: Images of cells showing co-localization of DRneo (FITC, green signal) and γH2AX, Ku86, DNA ligase IV, DNA ligase IIIα and WRN (TRITC, red signal) in NC10DRneo cells transfected with ISce1. Nuclei are stained with DAPI (blue). Right panels are merged images of FITC and TRITC showing co-localization.
B: Histogram showing the percentage of co-localization in both K562DRneo (black bar) and NC10DRneo cells (gray bar).

Supplementary Figure 3

Viability (%) measured using trypan blue dye exclusion

A

K562	Viability (%)
siRNA Nontarget	95%
siRNA WRN	91%
siRNA DNA ligase IIIα	87%

B

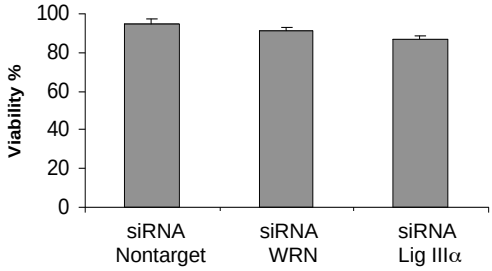

A: Table of % viability in siRNA Nontarget, siRNA WRN and siRNA DNA ligase IIIα experiment in K562 cells.
B: Histogram showing the percentage of cell viability. Error bars reflect the standard error of the mean.

Supplementary Table 1

Patient Samples 46,XX,t(9:22)(q34:q11.2)	% of BCR-ABL Positive Cells	Gleevec Treatment mg/day	White Blood Count (WBC) 10^9/l
CML1	60	400	12290
CML2	100	400	30640
CML3	100	400	24144
CML4	100	600	14210

BCR-ABL cells were measured by FISH.
>100 cells were examined.
All samples were bone marrow mononuclear cells (MNC).
The duration of Gleevec treatment at the time of sampling was between 6 and 12 months.

Supplementary Table 2

γ-H2AX foci formation in siRNA treated K562 with and without IR

	Total No. cells examined	>5 Foci
siRNA Nontarget no IR	302	14 (5%) ±1
siRNA Nontarget with IR	228	73 (32%) ±1
siRNA WRN no IR	204	36 (18%) ±1
siRNA WRN with IR	192	72 (38%) ±3
siRNA DNA ligase IIIα no IR	205	35 (17%) ±1
siRNA DNA ligase IIIα with IR	205	115 (56%) ±5

± Standard errors from three independent experiments.

Supplementary Table 3

***In vivo* Plasmid end-joining Assay in siRNA Treated K562**

siRNA treated K562 CML cells transfected with linearized pUC18 plasmid	No. of Blue Colonies	No. of White Colonies	*Total No. of Colonies	** Frequency Of Misrepair (%)	*** Large Deletions (%)
siRNA Nontarget	112	24	136(100%)	18±2	22±3
siRNA WRN	50	10	60(45%)	16±4	56±4
siRNA DNA ligase IIIα	24	14	38(28%)	37±4	20±1

*****Total no. of Colonies: The sum of blue plus white colonies is a measure of the efficiency of end-joining.

****** Frequency of Misrepair: Percentage of white colonies divided by total no. of colonies.

******* Large Deletions: Percentage of large deletions (>20bp) divided by total misrepared colonies examined.

± Standard errors from three independent experiments.